YALE PEABODY MUSEUM

JOURNAL OF MARINE RESEARCH

The *Journal of Marine Research,* one of the oldest journals in American marine science, published important peer-reviewed original research on a broad array of topics in physical, biological, and chemical oceanography vital to the academic oceanographic community in the long and rich tradition of the Sears Foundation for Marine Research at Yale University.

An archive of all issues from 1937 to 2021 (Volume 1–79) are available through EliScholar, a digital platform for scholarly publishing provided by Yale University Library at https://elischolar.library.yale.edu/.

Requests for permission to clear rights for use of this content should be directed to the authors, their estates, or other representatives. The *Journal of Marine Research* has no contact information beyond the affiliations listed in the published articles. We ask that you provide attribution to the *Journal of Marine Research.*

Yale University provides access to these materials for educational and research purposes only. Copyright or other proprietary rights to content contained in this document may be held by individuals or entities other than, or in addition to, Yale University. You are solely responsible for determining the ownership of the copyright, and for obtaining permission for your intended use. Yale University makes no warranty that your distribution, reproduction, or other use of these materials will not infringe the rights of third parties.

Circulation and water masses of the southwest Pacific: WOCE Section P11, Papua New Guinea to Tasmania

by Serguei Sokolov[1] and Stephen Rintoul[1]

ABSTRACT

The circulation near the western boundary of the South Pacific is described on the basis of water properties and geostrophic velocities measured on a meridional section along 155E through the East Australian and Coral Basins. The section was occupied in winter 1993 as part of the World Ocean Circulation Experiment (WOCE, Section P11S). The primary objective of P11 was to quantify the zonal flows entering and leaving the western boundary of the basin.

The primary inflow to the Tasman and Coral seas is supplied by the South Equatorial Current (SEC), which crosses the P11 section as a wide band of westward flow between 14 and 18S with a total geostrophic transport of 55 Sv (1 Sv = 10^6 m³/s) relative to the bottom. The SEC bifurcates at the Australian coast near 18S: 29 Sv turns south to feed the East Australian Current (EAC), and 26 Sv recirculates in the Gulf of Papua New Guinea as a low-latitude western boundary current (the Great Barrier Reef and New Guinea Coastal Undercurrents, GBRUC/NGCUC). The NGCUC closes the tropical gyre, and carries South Pacific water around the Louisiade Archipelago and through the Solomon Sea to the equator.

The core of the EAC lies over the continental slope between 18S and 30S. A system of deep-reaching, recirculating eddies or gyres is located offshore of the EAC. At 30S the EAC separates from the coast, and the steeply sloping isopycnals associated with the current persist from the surface to the bottom. The total geostrophic transport of the EAC after separation is 57 Sv relative to the bottom. After separation from the coast, more than half of the EAC (33 Sv) recirculates north and then west, crossing P11 again at 28S. The remainder (24 Sv) continues east as a meandering jet across the Tasman Sea (the Tasman Front).

The circulation in the southern part of the Tasman Sea is dominated by transient eddies and standing gyres. An anticyclonic circulation facilitates the exchange of water between the Tasman Sea and the Southern Ocean. About 10 Sv of subantarctic water spreads north to 36–38S, then recirculates back to the west to merge with a weak southward flow of modified subtopical water near the Tasmanian coast. The circulation in the deeper layers consists of a weak northward deep western boundary current, a cyclonic recirculation filling the Tasman Basin, and a net export of about 3 Sv of deep water to the Coral Sea.

The transport of mode and intermediate water in the low-latitude western boundary current crossing P11 is similar to the transport in these density classes further "upstream" in the subtropical gyre at 32S. This suggests that the mode and intermediate waters entering the Pacific from the south to compensate the export through the Indonesian passages are carried north to the tropical western Pacific primarily along isopycnals.

1. CSIRO Marine Research and Antarctic Cooperative Research Centre, Hobart, Tasmania Australia. *email: serguei.sokolov@marine.csiro.au*

1. Introduction

Our present understanding of the circulation of the South Pacific is based on sparse historical data and only a few direct velocity measurements. The data have been particularly inadequate along the western boundary of the South Pacific, where the variability of the flow can be as energetic as the mean (Hamon, 1965; Boland and Hamon, 1970; Boland and Church, 1981). An accurate description of the circulation near the western boundary is critical to understanding the subtropical gyre as a whole, its exchange with subantarctic and tropical circulation regimes, and the ocean's role in the transport of heat, freshwater and biogeochemical properties.

The majority of the hydrographic stations occupied in the Tasman/Coral seas have been shallow (<1500 m deep). As a result, there has been little discussion of the deep circulation. The fact that most of the hydrographic data collected have been shallow has also meant that most geostrophic transport estimates have assumed a level of no motion at 1500 m depth or shallower, although the shear of the EAC extends to great depth and the few direct velocity estimates that do exist show strong flows at depth in the same direction as the near-surface currents (e.g. Boland and Hamon, 1970; Mulhearn *et al.,* 1988).

The recent deep hydrography which has been collected is either limited to particular regions of the Coral/Tasman seas, or consists of zonal sections which, while useful for the study of strong meridional flows like the EAC, are not appropriate for study of the zonal flows supplying and exporting water from the system of western boundary currents of the South Pacific.

To address these gaps in measurements of the southwest Pacific, a meridional section along 155E from Papua New Guinea to 43S was occupied as part of the World Ocean Circulation Experiment (WOCE) one-time survey (section P11) in the winter of 1993 (Fig. 1). The P11 section is the first synoptic, full-depth, meridional section through the deepest parts of the Tasman and Coral seas. The primary objectives of this analysis of P11 are to describe the water masses of the southwest Pacific, to quantify the top-to-bottom circulation of the Coral and Tasman seas with a particular focus on the zonal flows into and out of the western boundary, and to relate the circulation and water masses of the Coral and Tasman seas to the circulation of the South Pacific subtropical gyre as a whole.

We first briefly review the major circulation features of the southwest Pacific. In Section 3, the data used are described. In Section 4 we examine the water masses on P11 in some detail and use a number of supplementary data sets to place the P11 observations in the context of the South Pacific subtropical gyre. The circulation and transport of the Coral and Tasman seas are discussed in Section 5. We conclude with a summary of the main findings of the study.

2. Background

The inflow to the Coral Sea is supplied by the west-flowing South Equatorial Current (SEC) (Wyrtki, 1960; Reid, 1986; Fig. 1). The westward flow bifurcates at about 18S to
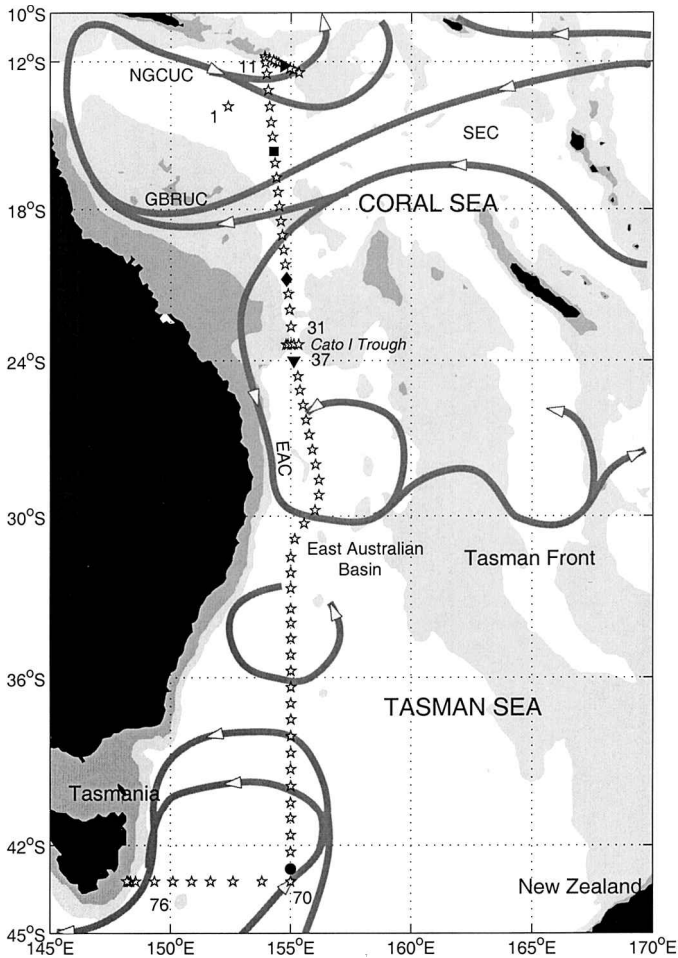
Figure 1. Position of the track of *Franklin 9306* (WOCE section P11). Light shading indicates depth shallower than 2500 m; dark shading indicates depth shallower than 250 m. Arrows indicate major circulation features of the southwest Pacific, as described in the text. The symbols other than stars (■, ●, ◆, and ▼) indicate stations used in Figure 12.

form northward and southward flowing boundary currents (Church, 1987). Church and Boland (1983) showed that the northward branch formed an undercurrent at a depth of 300–900 m offshore of the Great Barrier Reef. Godfrey (1989) and de Szoeke (1987) found that the presence of a northward western boundary current at these latitudes was implied by calculations of the wind-driven Sverdrup flow. Tsuchiya (1981), Lindstrom *et al.* (1987) and Tsuchiya *et al.* (1989) all inferred the presence of a continuous northward flow from the bifurcation at 18S along the boundary of the Coral Sea and into the Solomon Sea around the Louisiade Archipelago, but lacked the data to confirm its existence south of Papua New Guinea (PNG). Andrews and Clegg (1989) found eastward flow south of PNG,

which they took to be the northern branch of a weak cyclonic recirculation carrying 6 Sv in the upper 1000 m of the Gulf of Papua. Burrage (1993) also found a clockwise gyre in the Gulf of Papua in his analysis of several synoptic sections occupied in 1990, but estimated a much larger transport of 35 Sv above 1500 m.

The southward branch of the bifurcation at 18S feeds the East Australian Current (EAC), the intense but highly variable western boundary current of the South Pacific subtropical gyre. Due to the energetic variability, the transport of the EAC is not well defined. Most previous studies have relied on shallow (<1500 db) hydrographic data within 500 km of the coast and, in the absence of direct velocity measurements, have assumed a reference level at 1300 db or shallower (e.g. Hamon, 1965; Boland and Hamon, 1970; Boland and Church, 1981; Nilsson and Cresswell, 1981; Church, 1987). However, the few direct velocity measurements made in the EAC suggest the Current extends much deeper than 1300 db. For example, Boland and Hamon (1970), using direct measurements of current velocities from Swallow floats, showed that the total transport of the EAC is about two times higher than one estimated with a reference level of 1300 db. Mulhearn *et al.* (1988) used electromagnetic measurements to confirm that absolute transports are greater than geostrophic transports relative to 1300 m by a factor of approximately 1.6.

The EAC separates from the coast between 30S and 35S (Wyrtki, 1962b; Godfrey *et al.,* 1980). After separation, part of the EAC turns offshore in a meandering eastward jet known as the Tasman Front (Andrews *et al.,* 1980). The Tasman Front can be traced as a continuous feature from the separation of the EAC to the northern tip of New Zealand, although the net transport associated with the front is difficult to determine due to the presence of energetic eddies (Andrews *et al.,* 1980; Stanton, 1981). Stanton (1981) estimated the transport of the Tasman Front to be 12–13 Sv relative to 1300 db, based on a detailed synoptic XBT survey, roughly comparable to the mean transport of 13–15 Sv in the upper 500 m observed between New Zealand and Fiji by Morris *et al.* (1996). Warren (1970) suggested that such a zonal jet was required to link the EAC to the southward flow east of New Zealand to form a continuous boundary current along the western boundary of the subtropical South Pacific.

The maps by Wyrtki (1962b) and Reid (1986) show that the EAC can be divided into three components after separating from the coast. In addition to the eastward branch described above, some portion of the flow turns to the north and recirculates, and a third branch continues southward past Tasmania. The Sverdrup calculations of de Szoeke (1987) and Godfrey (1989) imply a transport of about 12 to 17 Sv out of the Tasman Sea to the south across 43S, while Wyrtki (1962b) estimates a southward flow of 13 Sv between the surface and 1200 m depth (relative to 1750 m), and Ridgway and Godfrey (1994) find a net outflow above and relative to 2000 m of 7 Sv. The extent to which this southward flow turns to the west south of Tasmania, as suggested by Reid's (1986) maps, or turns to the east off Tasmania as suggested by Stramma *et al.* (1995), is unknown.

South of the EAC separation point the circulation in the western part of the Tasman Sea is dominated by a very intense eddy field. Warm-core anticyclonic eddies are formed by pinching-off of poleward EAC meanders, and may coalesce with the EAC again (Nilsson *et al.,* 1977; Andrews and Scully-Power, 1976; Nilsson and Cresswell, 1981). The observations summarized by Nilsson and Cresswell (1981) suggest that warm-core EAC eddies, once formed, can remain in the same place for several months and have a life time as long as 650 days. These eddies extend from the surface to abyssal depths, and the total recirculating transport of a single ring may be as large as 100 Sv (Lilley *et al.,* 1986).

Farther south the Subtropical Front (STF, also called the Subtropical Convergence) marks the boundary between warm, salty subtropical waters to the north and cool, fresh subantarctic waters to the south (Wyrtki, 1962a). The STF is generally limited to the upper few hundred meters of the ocean and changes in temperature and salinity across the front are nearly density-compensating (Rintoul and Bullister, 1999), hence the transport of the STF is small (3 Sv, Stramma *et al.,* 1995). The STF is generally found between 40S and 45S in the Tasman Sea, although the position of the front varies on a range of time scales. Some of the warm water carried south by the EAC may leave the coast to the east along this front. The location of the front in the eastern Tasman Sea is debated in the literature, in part the result of different definitions of the front being used by different authors. Wyrtki (1962a) and Deacon (1937) showed the STF stretching northeast from southern Tasmania toward the North Island of New Zealand. Garner (1959, 1967), Heath (1985), and Stramma *et al.* (1995), on the other hand, concluded that the Subtropical Front extends southeast toward the southern tip of New Zealand.

Details of the deep circulation in the Coral and Tasman seas are sketchy. Wyrtki (1961) showed that the abyssal waters of the East Australian Basin were of circumpolar origin, but did not discuss details of the flow. Warren (1973) concluded that the flow of deep water in the Tasman Sea must be extremely sluggish, and that higher deep salinities at 28S relative to 43S could only be explained by assuming temporal variations in the salinity maximum water entering the basin from the south. Reid (1986) argued for a more vigorous cyclonic deep flow in the Tasman Sea, with an equatorward deep western boundary current off Australia. Reid cautioned, however, that the cyclonic flow was in part the result of the large bottom velocities (2–4 cm/s) he was led to assume in order to agree with the tracer patterns, and that the data coverage for accurate calculation of the deep circulation in the Tasman and Coral seas was inadequate.

Wyrtki (1961) concluded from potential temperature-salinity relationships that relatively high salinity Coral Sea deep water must have come from the East Australian Basin. Lindstrom and Hayes (1989) confirmed Wyrtki's picture of a generally south to north flow from the East Australian Basin through the Coral Sea to the Solomon Basin. Lindstrom and Hayes noted that the influence of Central Pacific Deep Water in the southern Solomon Basin was more widespread than suggested by Wyrtki. They could not determine, without

additional observations, whether the Central Pacific Deep Water could also reach the northern Solomon Basin through the Solomon Trench.

3. Data

WOCE section P11 was carried out on R/V *Franklin* in June–July 1993. A total of 80 stations were occupied (Fig. 1). On each station a rosette sampler equipped with a CTD was lowered to within 10 m of the sea floor. Stations were spaced generally at intervals of 66 km, but at closer intervals (about 10–15 km) near the Tasmania and Papua New Guinea coasts, and across the Cato Island Trough. Continuous profiles of temperature, salinity and oxygen were obtained at each station, and water samples at 24 depths were analzyed for salinity, oxygen and nutrients. (The nutrient data are not discussed in this paper.) Continuous underway measurements of velocity were obtained with a 150 kHz acoustic Doppler current profiler (ADCP).

A number of other data sources were used to complement the 1993 *Franklin* cruise. The portion of P11 along 43S was occupied by RSV *Aurora Australis* in April 1993, with full-depth casts at the same station locations as the *Franklin* cruise 3 months later (Rosenberg *et al.,* 1995). These data are used to confirm our estimates of geostrophic circulation and water mass properties along the southern boundary of the Tasman Sea. To derive a complete picture of the Coral Sea water mass properties, several recent cruises in the Coral and Solomon seas have been used, including *Franklin* cruises in 1985, 1988 and 1990, and two cruises from the WEPOCS expedition (Lindstrom *et al.,* 1987). Some results from the *Franklin* cruises have been published by Andrews and Clegg (1989) and Burrage (1993).

To place the observations in the southwest Pacific in the context of the overall circulation of the subtropical gyre of the South Pacific, maps of water properties and dynamic topography were prepared, based on a new hydrographic data set for the South Pacific (SPAC) which includes some WOCE and historical data (Gouretski and Jancke, 1996). The data were kindly provided by Victor Gouretski and Kai Jancke. The original station data were averaged on neutral density surfaces following the recommendations made by Lozier *et al.* (1994), and the maps were prepared using the methods described in Sokolov and Rintoul (1999). All the data were labeled with the neutral density variable using the software written by David Jackett (Jackett and McDougall, 1994); density values quoted in the text are neutral density, in units of kg/m^3.

4. Water masses of the southwest Pacific

Equatorward of the Subtropical Front, the near-surface layers in the western South Pacific consist of Tropical Surface Water (TSW), with high temperature and low salinity, and Subtropical Lower Water (SLW), which forms a salinity maximum (Wyrtki, 1962a). Poleward of the STF, and equatorward of the Subantarctic Front (SAF), the Subantarctic

Mode Water (SAMW) is formed by deep winter convection and is identified by a high oxygen pycnostad (McCartney, 1977). The Antarctic Intermediate Water (AAIW), characterized by a salinity minimum, occupies the intermediate layer just below the SAMW. SAMW and AAIW are exported from the Southern Ocean into the subtropical gyres, where they renew the waters of the lower thermocline (McCartney, 1982). An oxygen minimum is found throughout the South Pacific near a depth of about 2000 m. Low oxygen water spreads from the Pacific to the Southern Ocean, where it contributes to the Upper Circumpolar Deep Water (UCDW) layer (Callahan, 1972). The Lower Circumpolar Deep Water (LCDW), characterized by a weak salinity maximum, is a last remnant of the North Atlantic Deep Water, which can be detected in the Pacific Ocean as far as 10N (Reid and Lynn, 1971). The LCDW is found in the South Pacific at depths between 2500 and 3000 m. The abyssal waters are cool and fresh relative to the overlying LCDW, reflecting the input of modified Antarctic Bottom Water (AABW).

In the following section, each of these water masses is considered in turn. The distribution of water masses is determined from vertical sections of water mass properties and water mass anomalies; the latter are particularly useful for identifying deep-reaching property fronts associated with the flow field. Basin-wide maps of properties on particular core layers or isopycnals are used to relate the features observed on P11 to the circulation of the subtropical gyre as a whole. The circulation paths inferred from a detailed look at the water mass properties along P11 are used to constrain the transport estimates presented in Section 5.

a. Subtropical Lower Water

The Subtropical Lower Water is present throughout the region and is characterized by a high salinity core located between the surface and 200 m depth (Fig. 2b). Two varieties of SLW have been described in the western part of the South Pacific (Wyrtki, 1962a; Donguy and Henin, 1977). A warm, salty variety is found north of Fiji and the New Hebrides, and a cool, fresh variety is situated north of New Zealand.

i. Northern component of the SLW. On P11, the salinity maximum of the northern component is found in the upper thermocline at 100 to 200 m depth north of about 25S, with density between 24.4 and 24.8, temperature between 21 and 25°C, and salinity of 35.7 (Fig. 2).

The warm and salty northern variety of SLW is formed in the central South Pacific near the Society Islands (12 to 25S, 100 to 150W) (Donguy and Henin, 1977; Donguy, 1994). A surface salinity maximum with salinity greater than 36.8 (Fig. 3) coincides with a maximum in evaporation minus precipitation of more than 100 W/m^2 (129 cm/yr) in this region (Weare *et al.,* 1981). Donguy (1994) showed that the subsurface salinity maximum of the SLW in the western South Pacific was the result of these high salinity surface waters being carried west in the northern arm of the subtropical gyre and under-riding lighter, low
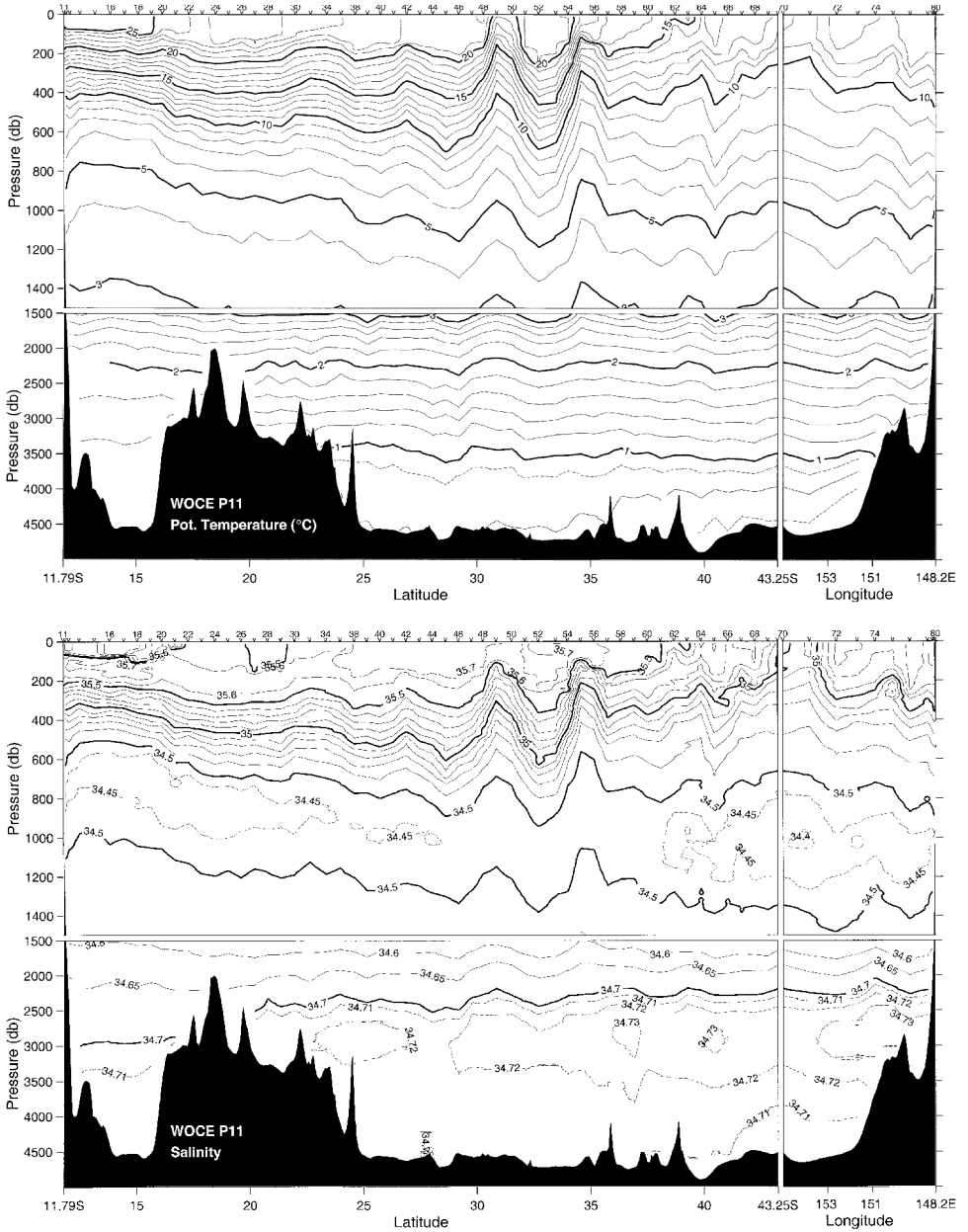
Figure 2. Vertical sections of water properties along WOCE section P11. The section turns at 43S, and runs west to the coast of Tasmania. Station locations are indicated by ''v'' and station numbers at top of plot. (a) Potential temperature (°C) (contour interval 1°C (0.2°C) above (below) 1500 db); (b) salinity (contour interval 0.1 (0.05) above (below) 1500 db); (c) oxygen (μmol/l) (contour interval 10 μmol/l); (d) neutral density (kg/m³) (contour interval 0.1 (0.05) above (below) 1500 db).
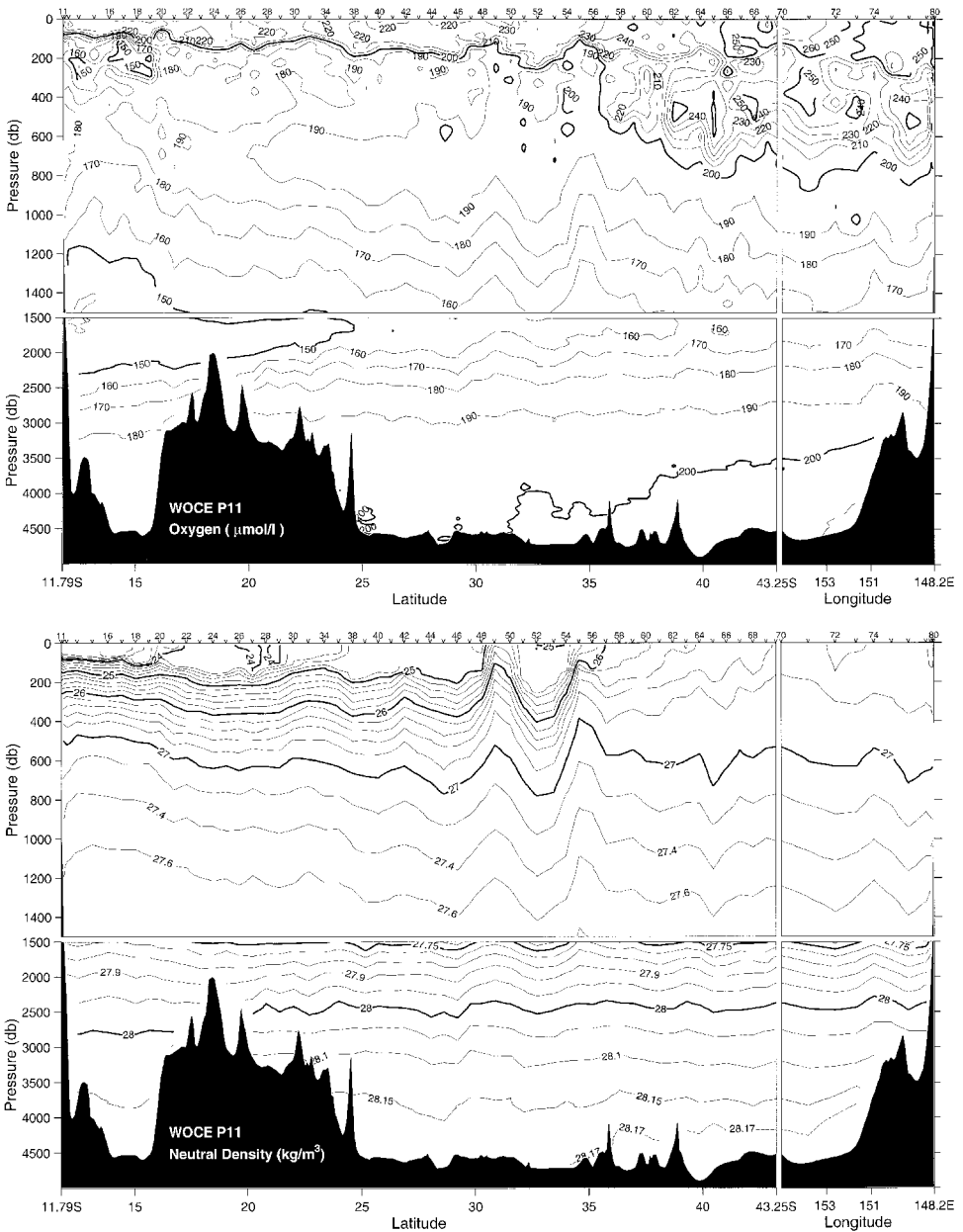
Figure 2. (Continued)

salinity water produced by an excess of precipitation over evaporation in the western tropical Pacific. Due to mixing and oxygen consumption, the salinity and oxygen of the northern SLW decrease from east to west from 36.5 to 35.8 and from 5.0 to 3.75 ml/l (224 to 168 μmol/l), respectively (Fig. 4).
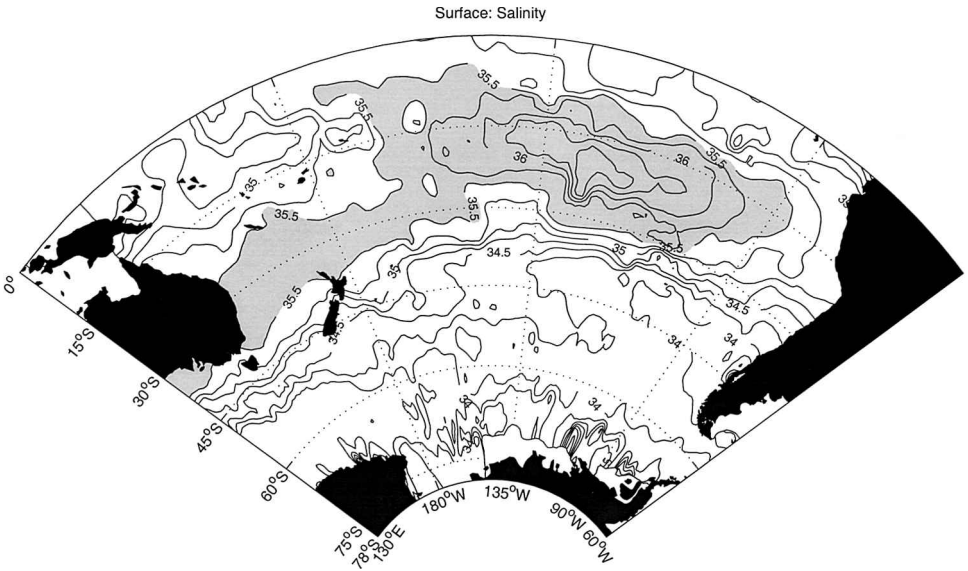
Surface: Salinity

Figure 3. Salinity of the sea surface. Shading indicates salinity higher than 35.5.

The northern boundary of the high salinity tongue of the SLW runs from north of the Society Islands to just north of the Solomon Islands, along about 5S (Fig. 4). The horizontal gradients across the northern boundary are very strong, with salinity differences of about 0.2–0.6. Salinity gradients across the southern boundary, near 15S, are smaller. Oxygen on the salinity maximum increases from north to south and does not coincide with the salinity distribution in this core layer. At P11, the oxygen increase to the south occurs as a sharp front at 16S, with oxygen at the salinity maximum increasing from $<150\,\mu$mol/l to $>180\,\mu$mol/l across the front, while the salinity freshens to the south by 0.06 (Figs. 2, 5).

Donguy (1994) argued that the sharp salinity front near 5S in Figure 4a marks the boundary between newly-formed SLW spreading westward in the SEC south of 5S and modified SLW returning to the east in the Equatorial Undercurrent (EUC) farther north. The modified SLW is lower in salinity and oxygen due to mixing and oxygen consumption along this path. Results of the WEPOCS expedition show that the primary source of the EUC in the western Pacific is the New Guinea Coastal Undercurrent, (NGCUC) which transports high-salinity, high-oxygen, low-nutrient water (including SLW) from the Solomon and Coral seas through Vitiaz Strait to the equator (Lindstrom *et al.,* 1987; Toole *et al.,* 1988; Tsuchiya *et al.,* 1989). Another branch of the westward flow carrying SLW passes north of the Solomon Islands and feeds the EUC north of New Ireland. This branch also carries high-salinity water, but the oxygen content is lower compared with waters coming through the Coral and Solomon seas (Tsuchiya *et al.,* 1989; Butt and Lindstrom, 1994).

The distribution of salinity and oxygen in the core layer of the SLW (Fig. 4) clearly shows this circulation pattern. A low-oxygen tongue (<3.0 ml/l, 130 μmol/l) passes north

of the Solomon Islands. Salinity maximum water of intermediate oxygen concentrations (3.5–3.75 ml/l, 158–168 μmol/l) enters the Coral Sea between the Solomon Islands and Vanuatu. SLW with even higher oxygen concentrations (>4 ml/l, 180 μmol/l) appears to enter the Coral Sea between Vanuatu and New Caledonia. The sharp oxygen front at 16S on P11 (Figs. 4, 5) marks the boundary between the intermediate oxygen SLW entering the Coral Sea north of Vanuatu and the higher oxygen SLW entering the basin south of Vanuatu.

The inference of significant inflow to the Coral Sea between Vanuatu and New Caledonia based on the oxygen distribution conflicts with the circulation map of Andrews and Clegg (1989), which shows little net flow in this region. However, the oxygen distribution and geostrophic velocities relative to the bottom along an unpublished 1985 R.V. *Franklin* section indicates a strong inflow of about 25 Sv between Vanuatu and New Caledonia. Westward flow in subsurface layers of relatively high oxygen (180 μmol/l) SLW ($\gamma_n \sim$24.4–24.8) between Vanuatu and New Caledonia was also inferred by Wyrtki (1962b). The oxygen front near 16S on P11 is a continuation of the oxygen front located at 15S just north of Vanuatu. These patterns in the oxygen distribution are consistent with those presented by Wyrtki (1962a). Thus we can conclude that there is strong inflow to the Coral Sea both south and north of Vanuatu, with the southern branch carrying higher oxygen SLW.

ii. Southern component of the SLW. South of 25S on P11 (station 38) the salinity maximum reaches the sea surface, marking the northern boundary of the cooler, fresher, denser southern variety of SLW. Because the SLW outcrops in winter in the Tasman Sea, it is higher in oxygen than the northern component of SLW on P11. The southern boundary of the southern SLW on P11 is marked by the strong near-surface horizontal salinity gradient associated with part of the Subtropical Front at 38S (station 61). The southern variety of SLW on P11 is characterized by temperatures between 16 and 22°C, salinities between 35.5 and 35.7, and densities between 24.8 and 26.3 (Fig. 2).

Wyrtki (1962a) suggested that the southern component of the SLW enters the Tasman Sea from the east between New Zealand and Fiji and then sinks along the Tropical Convergence toward the north. In contrast, Donguy and Henin (1977) argued that because the surface flow between New Zealand and Fiji is mainly eastward south of 23S, the southern component must originate somewhere in the Tasman Sea. Similarly, Morris *et al.* (1996) found that the flow in the upper 800 m south of about 20S is eastward.

The distributions of salinity and potential temperature on the isopycnal corresponding to the core layer of southern SLW ($\gamma_n = 25.4$) are almost flat over the entire western part of the South Pacific (Fig. 6a). The oxygen distribution, on the other hand, reveals some patterns which can be interpreted in terms of circulation (Fig. 6b).

A low-oxygen tongue spreading southward along the western boundary of the Tasman Sea can be clearly identified as the EAC. Apart from an indication of a return flow to the north located west of New Caledonia, there is no clear indication of strong meridional
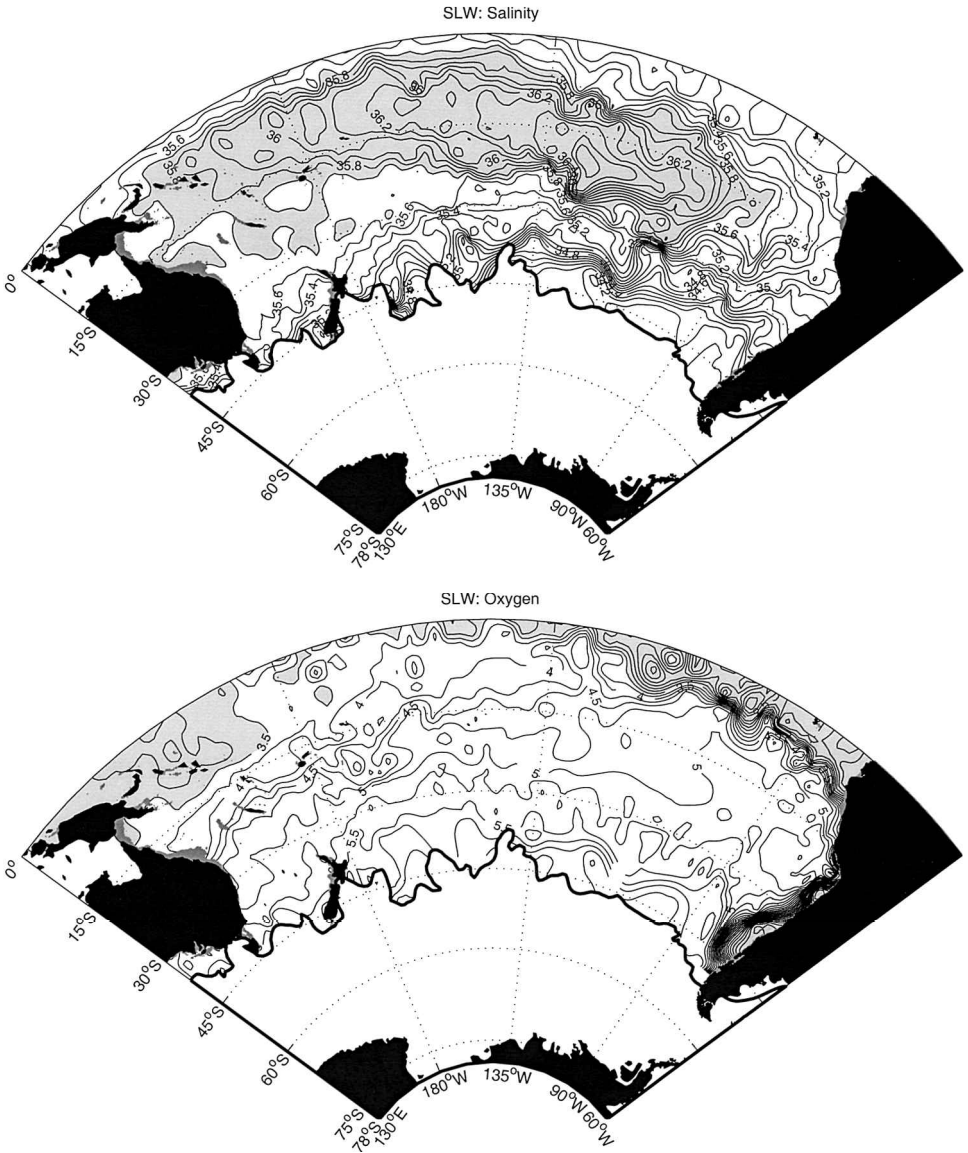
Figure 4. Properties in the upper salinity maximum of the Subtropical Lower Water. (a) salinity (shading indicates salinity higher than 35.7). (b) oxygen (ml/l) (shading indicates oxygen lower than 3.5 ml/l).

advection across the Tropical Convergence toward the north. A sharp meridional gradient in oxygen runs across the entire South Pacific, coincident with the position of the Tropical Convergence, indicating that the northward subduction of the high-oxygen southern SLW across the front due to Ekman pumping is a relatively slow process. The configuration of
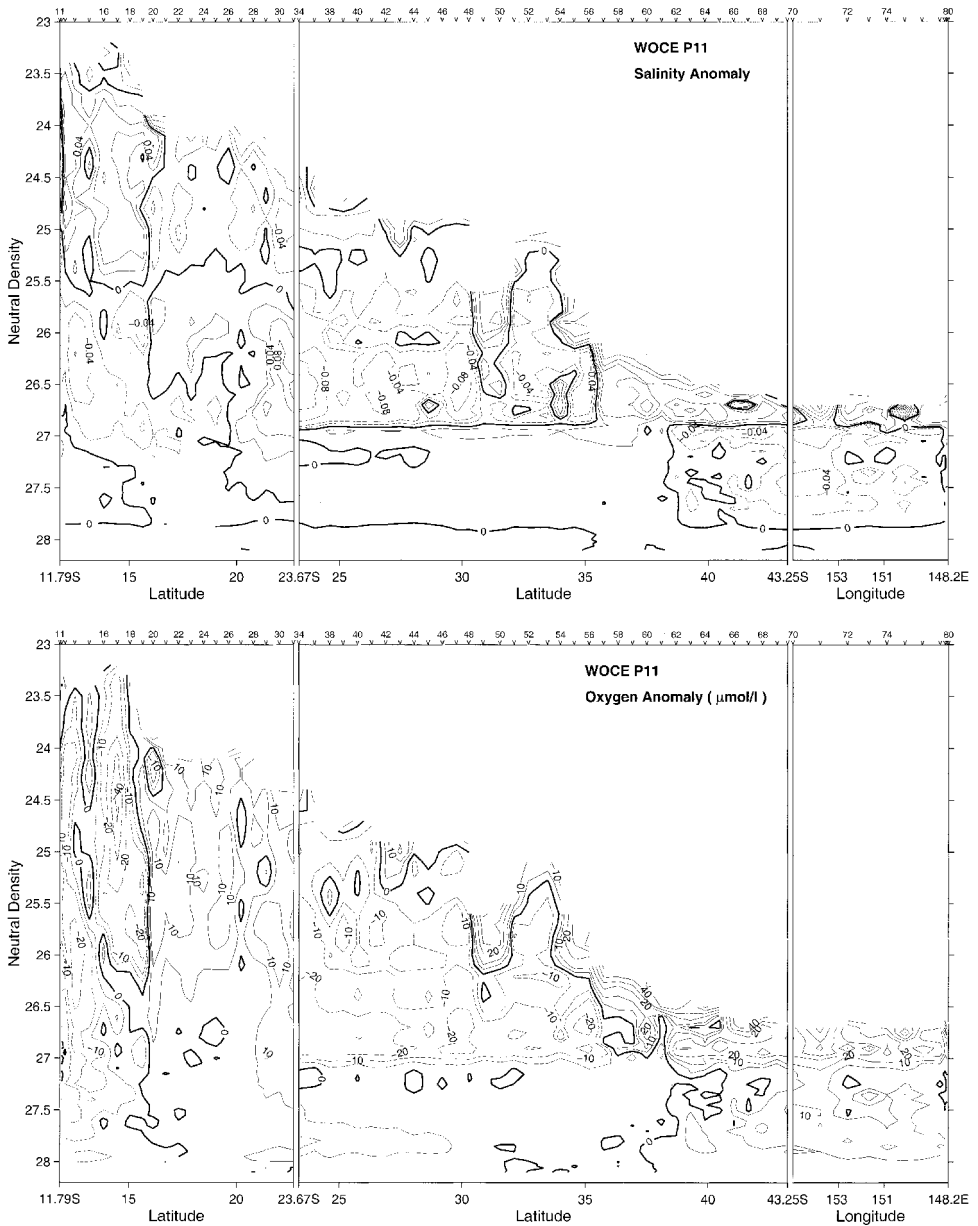
Figure 5. Water property anomalies along WOCE section P11 plotted in neutral density coordinates. Anomalies are defined relative to the mean profile for stations in the Coral Sea (left panel) and in the Tasman Sea (middle and right panels). Positive values are higher in salinity or oxygen than the mean profile. (a) salinity anomaly, (b) oxygen anomaly.

SLW, gamma$_n$=25.40: Salinity
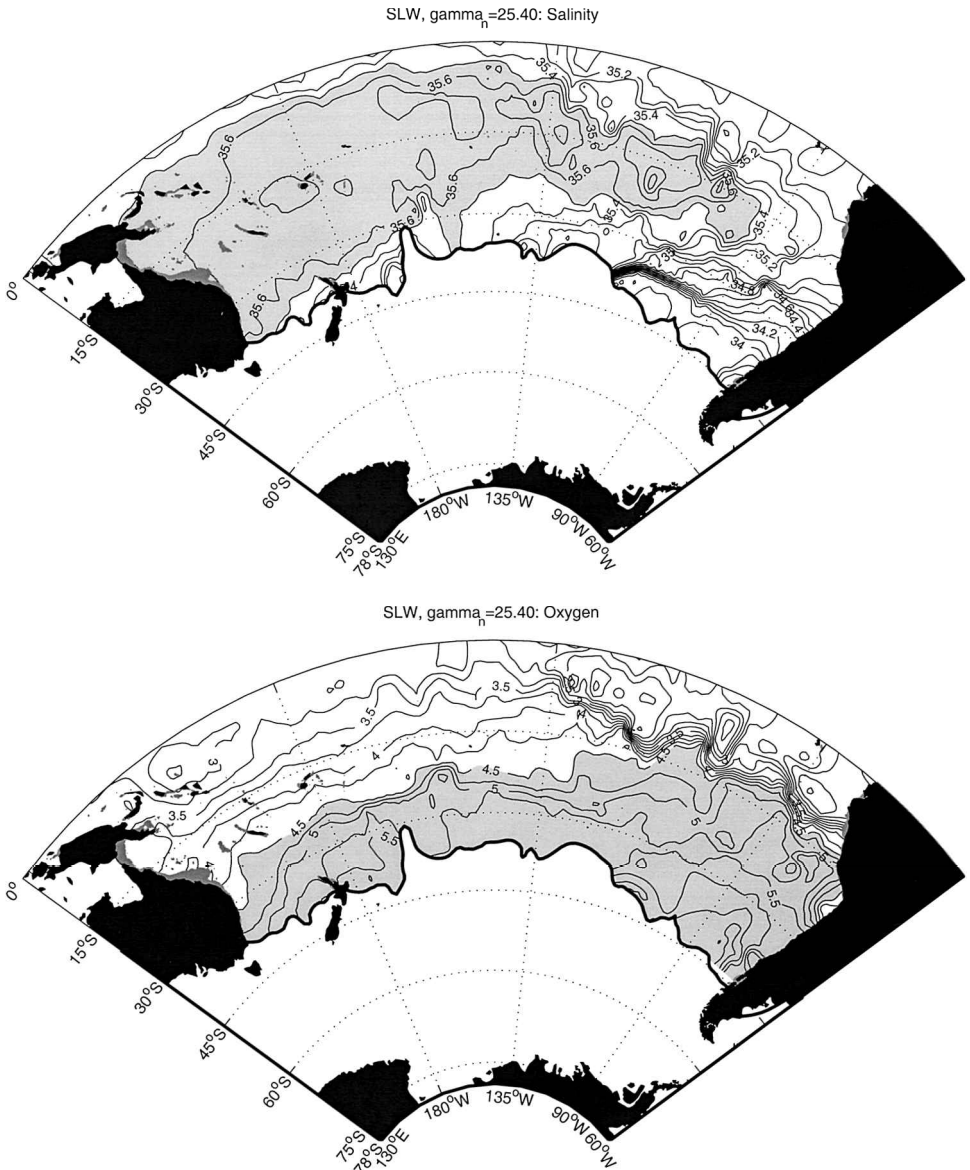

SLW, gamma$_n$=25.40: Oxygen

Figure 6. Water properties on the isopycnal corresponding to the southern component of the Subtropical Lower Water ($\gamma_n = 25.40$). (a) salinity (shading indicates salinity higher than 35.5), (b) oxygen (ml/l) (shading indicates oxygen higher than 4.5 ml/l).

the oxygen front is similar to the schematic depiction of "a northern current band near 30S" presented by Stramma *et al.* (1995), with about a 2–3° southward shift of the current band relative to the front.

As found for the northern type of SLW, the formation region of the southern type of

high-salinity SLW—the central Tasman Sea—coincides with a maximum excess of evaporation over precipitation (>50 W/m^2, 65 cm/yr; e.g. Weare *et al.,* 1981, Fig. 13). This region also experiences strong cooling by the atmosphere in the annual mean (more than 60 W/m^2), driving winter convection. Deep mixing during winter increases the oxygen content of the surface layer. The effect of winter convection can be clearly seen in Figure 2, with maximum mixed layer depths of more than 200 m depth found equatorward of the separated EAC and within the warm-core EAC eddy. Southern SLW is supplied by the lighter, northern variety of SLW, which spreads to the south and upward along the sloping isopycnals, as seen clearly in the upper 200 m on P11. When this water outcrops in winter in the central Tasman Sea, it is converted to the southern variety of SLW by loss of heat and freshwater to the atmosphere. The transport estimates in density layers discussed in Section 5 show a net convergence of about 5 Sv of northern SLW, which is balanced by a net export of southern SLW.

The maps of property distributions on the $\gamma_n = 25.4$ surface (Fig. 6) suggest that ventilated SLW carried eastward by the EAC spreads around the subtropical gyre of the South Pacific and is driven northward beneath the Tropical Convergence zone by Ekman pumping. The high-oxygen southern SLW under-rides the newly formed northern SLW in the central Pacific. Slightly higher temperature and salinity on the $\gamma_n = 25.4$ surface in the formation region of northern SLW (Fig. 6a) shows that vertical mixing in this region carries heat and salt downward to the underlying southern SLW. The two super-posed varieties of SLW are carried westward to the Coral Sea in the SEC along the northern flank of the subtropical gyre (Section 5). In the eastern Coral Sea the SLW spreads westward beneath a lighter water mass formed in the western equatorial Pacific, the Tropical Surface Water. Here the two components of SLW are separated by only 40–60 m in depth and become almost indistinguishable within the cyclonic gyre of the Coral Sea.

At densities of 25.6 to 26.6, the low-oxygen northern branch of the SEC is about 0.2°C cooler and 0.06 fresher compared to the waters carried by the SEC south of 16S (Fig. 5). This occurs due to poleward shift of the axis of the subtropical gyre in the upper 500 m. Water in the $\gamma_n = 23.6 - 25.6$ layer arrives at P11 from the formation region of the northern component of SLW (12S to 25S, 100W to 150W). Part of this SLW feeds the EUC. This SLW is modified by lateral mixing as it flows to the east in the EUC, and becomes fresher, cooler, denser (25.6–26.6), and lower in oxygen. Part of the modified SLW leaves the EUC near 180W and turns south to join the SEC. The front near 16S at densities of 25.6 to 26.6 marks the boundary between SLW of Tasman Sea origin to the south, and recirculated, modified SLW in the north.

iii. Subtropical mode water. The deep mixed layers formed on the equatorward side of the western boundary currents of the subtropical gyres are known as subtropical mode waters (STMW) (Schroeder *et al.,* 1959; Worthington, 1959). In the southwest Pacific, the STMW can be thought of as a subset of Wyrtki's broadly defined SLW. Roemmich and Cornuelle (1992) discuss the properties and distribution of the STMW of the South Pacific. They identify two modes, the stronger (i.e. thicker thermostad) having temperatures between 15°

and 17°C, the weaker having temperatures between 17° and 19°C. They note that the STMW of the South Pacific is much weaker than the mode waters of the northern hemisphere gyres, which likely reflects the small isotherm displacement across the relatively weak EAC compared to its northern hemisphere counterparts, the Gulf Stream and Kuroshio.

Roemmich and Cornuelle focused on measurements between New Zealand and Fiji, although the modes they identified there had a wider distribution. The mid-winter P11 section shows a well-developed thermostad with temperatures between 21° and 22°C, significantly warmer than the thermostads found north of New Zealand. The decrease in temperature of the STMW thermostad between the western Tasman Sea and the New Zealand-Fiji line likely reflects two factors: first, the warmer STMW is confined within a tight recirculation west of the Lord Howe Rise which is evident in the dynamic topography and property distributions discussed below; second, the STMW which does escape the recirculation is further cooled as it is advected to the east.

Tsuchiya (1981) argued that a much cooler STMW, the "13°C water," was formed in the southern Tasman Sea just north of the STF which, after a long transit around the subtropical gyre and through the Coral and Solomon seas, ultimately formed the thermostad of the Equatorial Undercurrent (EUC). Toggweiler *et al.* (1991), on the other hand, concluded from radiocarbon measurements that, while the water in the EUC did indeed originate in the southwest Pacific, the starting point was SAMW with a temperature of about 8°C. On P11 the 13° and 14°C isotherms do indeed outcrop north of the STF to form a weak thermostad between 40 and 43S. However, there is little evidence of a thermostad in this temperature range being exported from the Tasman Sea across the New Zealand—Fiji sections of Roemmich and Cornuelle (1991), contradicting the idea that the 13°C thermostad in the EUC is fed directly by the weak 13°C thermostad of the Tasman Sea. This is also consistent with the water properties discussed below which suggest that the southern Tasman Sea is largely a "cul de sac" with little net meridional advection across 38S.

b. Tropical Surface Water

The Tropical Surface Water (TSW) on P11 forms a thin surface layer north of 17S, with temperatures of about 25°C and salinities less than 35.1. The TSW originates at the surface in the western equatorial Pacific (Fig. 3), where heavy precipitation associated with the South Pacific Convergence Zone forms a shallow halocline, or "barrier layer," such that the depth of the surface isohaline layer is shallower than the isothermal layer (Lindstrom *et al.,* 1987).

The southern boundary of the TSW on P11 coincides with the subsurface oxygen front at 16S separating the northern and southern branches of the SLW entering the Coral Sea (Figs. 2, 5). The presence of a very light surface layer with neutral density less than 23.5 above the northern SLW enhances the density gradients in the upper thermocline. South of the oxygen front the southern SLW extends to the sea surface, and is not capped by a lighter

layer. It is likely that the low oxygen content of the northern branch of the SLW entering the Coral Sea results from suppressed oxygen influx from the surface due to the strong pycnocline which isolates the SLW from the sea surface. Comparison of P11 to 1985 R.V. *Franklin* cruises in the Coral Sea shows that the TSW was more widespread in 1985, but in both data sets the distribution of the low-oxygen component of SLW coincides with that of the TSW.

c. Subantarctic Mode Water (SAMW)

The Subantarctic Mode Water (SAMW) is formed by deep winter convection north of the Antarctic Circumpolar Current (ACC), between the STF and the SAF (McCartney, 1977). The deep mixing which forms SAMW imprints this water mass with its characteristic properties: high oxygen and a thick pycnostad (or layer of low potential vorticity). Using these water mass signatures, the SAMW can be traced from its formation region in the Southern Ocean as it spreads equatorward in the subtropical gyres. Due to its high oxygen content, the SAMW plays an important role in ventilating the lower thermocline of the southern hemisphere subtropical gyres (McCartney, 1982). SAMW formed in the Pacific spans a wide range of densities (from potential densities σ_θ of 26.9–27.0 in the west to 27.04–27.11 in the east), with the circulation of the lighter SAMW restricted to the southwest corner of the basin, while the denser SAMW is swept northwestward by the subtropical gyre circulation. The western varieties are much warmer and saltier (8.0–9.5°C and 34.60–34.75; Thompson and Edwards, 1981; Rintoul and Bullister, 1999) than the eastern varieties (4.3–5.1°C, 34.20; McCartney and Baringer, 1993). Modes with intermediate properties form in the subantarctic zone near New Zealand (Gordon, 1975), however their circulation is restricted to the area west of the East Pacific Rise.

Maps of properties on the SAMW isopycnal surfaces show the warm, salty, light varieties confined to the Tasman Sea and east of New Zealand, and the cool, fresh, dense SAMW formed in the southeastern Pacific (Figs. 7, 8). The tongue of southeastern Pacific SAMW spreads northwestward with the subtropical gyre circulation and bifurcates at 90W: a northern branch carries predominantly denser varieties of SAMW around the subtropical gyre to enter the Coral Sea north of Vanuatu, and a southern branch carries somewhat lighter varieties westward south of 35S. The southern branch does not appear on previously published maps based on more limited data (see e.g., Reid, 1965); however, McCartney and Baringer (1993) inferred its existence from the fact that the lighter modes which spread north across the Scorpio section at 43S did not appear on the 28S section, and so must have recirculated to the west south of 28S.

On P11 the SAMW forms a prominent pycnostad between 26.8 and 27.0 south of 38S (Fig. 2d), which coincides with a layer of high oxygen between 200 and 600 m depth (Fig. 2c). The SAMW does not outcrop on P11 so it must be advected from the formation region located farther south. In late winter the SAMW produced south of Tasmania forms a 600-m thick thermostad with temperatures of 8.5–9.5°C, salinities of about 34.60–34.75,

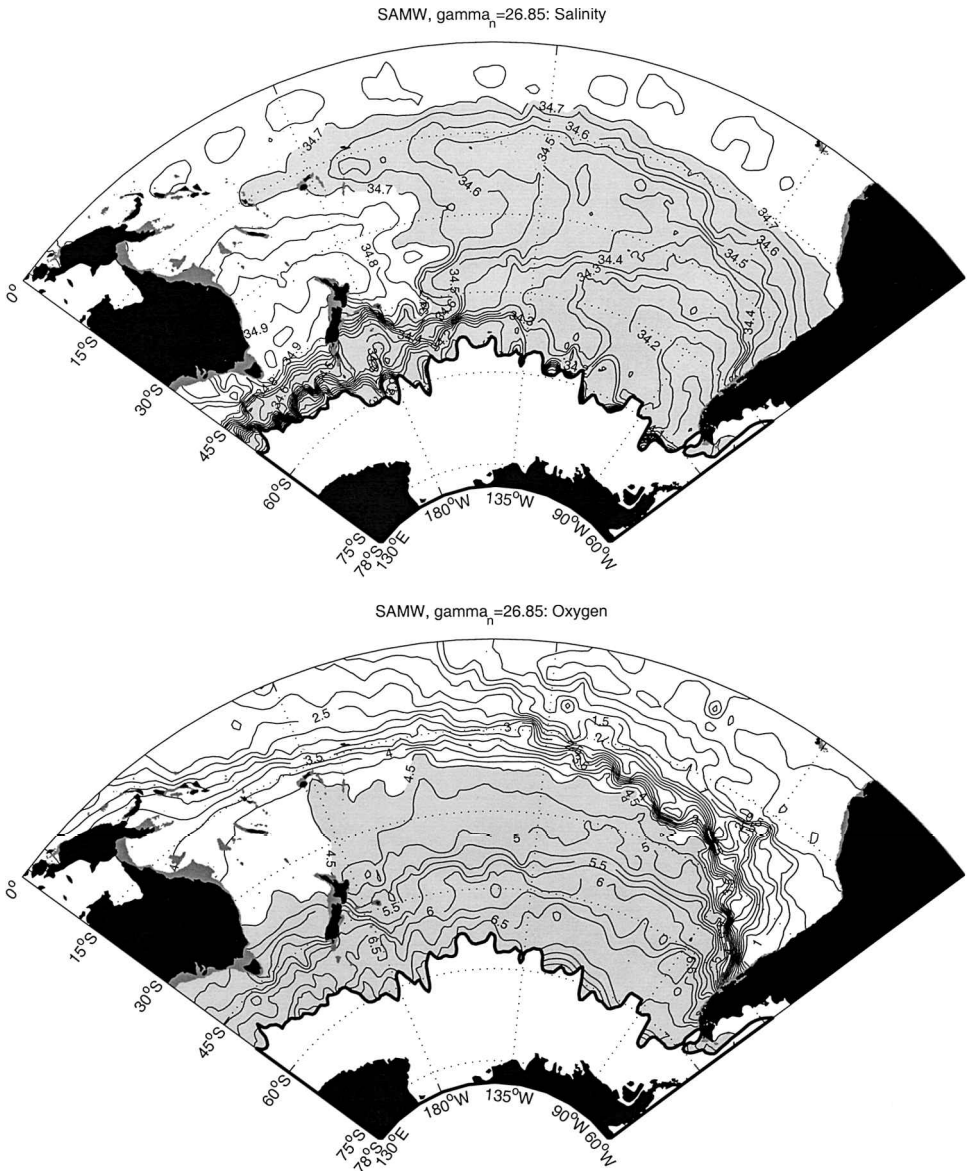SAMW, gamma$_n$=26.85: Salinity

SAMW, gamma$_n$=26.85: Oxygen

Figure 7. Water properties on the isopycnal corresponding to the Subantarctic Mode Water (SAMW) ($\gamma_n = 26.85$). (a) salinity (shading indicates salinity lower than 34.7), (b) oxygen (ml/l) (shading indicates oxygen higher than 4.5 ml/l).

and neutral densities of 26.8–27.0 (Thompson and Edwards, 1981; Rintoul and Bullister, 1999), similar in properties to the SAMW observed on P11.

The SAMW pycnostad is prominent on the 43S portion of P11, but it is not uniform along the section, reflecting flows entering and leaving the southern Tasman Sea (Fig. 2).
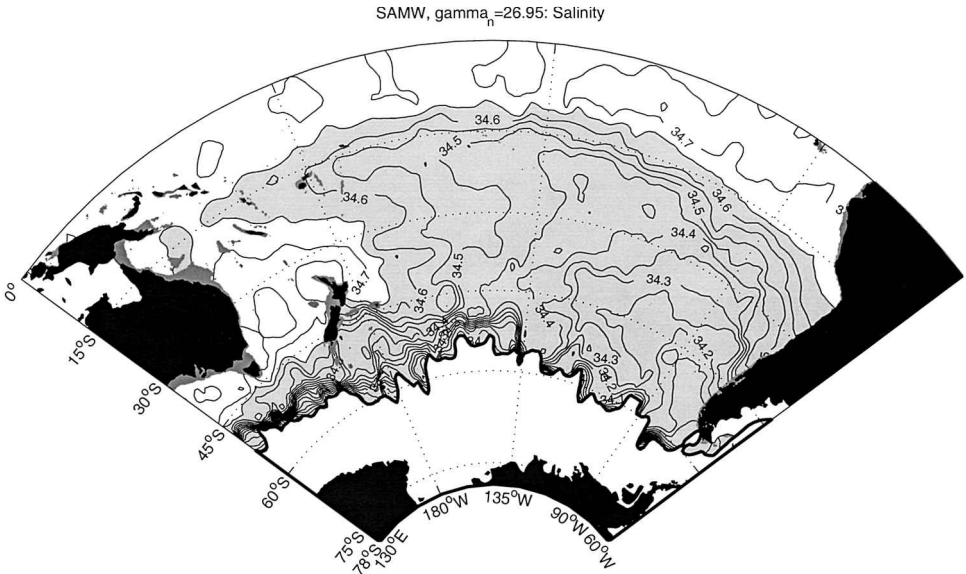
Figure 8. Salinity on the isopycnal corresponding to the Subantarctic Mode Water (SAMW) ($\gamma_n = 26.95$). Shading indicates salinity lower than 34.65.

The pycnostad is thickest and highest in oxygen at station 71, where the geostrophic velocities show northward flow (see Section 5), while the pycnostad is poorly developed and low in oxygen in the southward flow adjacent to the coast of Tasmania (inshore of station 78).

SAMW entering the Tasman Sea from the south extends as far north as 38S, where a strong front in all water properties is found between stations 56 and 57. To the south of the front, water on the neutral density surfaces 26.8–27.0 is higher in oxygen, saltier and warmer (Fig. 5). The difference in water properties across the front is large: greater than 0.8°C in temperature, 0.24 in salinity and 60 µmol/l in oxygen. Nevertheless, some influence of the lighter SAMW entering from the south can be seen as far north as 28S (e.g., the oxygen maximum and thicker layer of 26.7 to 26.9 water at station 45). Water from the south is entrained at the edge of anticyclonic EAC eddies, producing a "curtain" of higher oxygen water wrapped around the perimeter of the eddy (Fig. 2c). Slightly higher temperature (0.2°C), salinity (0.04), and oxygen concentrations (6 µmol/l) in the $\gamma_n = 26.0 - 26.8$ layer in the interior of the eddy relative to EAC characteristics (Fig. 5) are the result of mixing with the southern waters wrapped around the eddy.

The denser SAMW formed in the southeastern Pacific enters the Coral Sea north of Vanuatu and is carried westward across P11 by the SEC. The distribution of the two varieties of SAMW along P11 is best illustrated by comparing properties on the oxygen maximum core layer to properties on isopycnals corresponding to the two types. The "Australian" SAMW with neutral density of 26.95 is about 2°C warmer and 0.2 more saline than the southeast Pacific SAMW, with neutral density of 27.15 (Fig. 9a,b). The
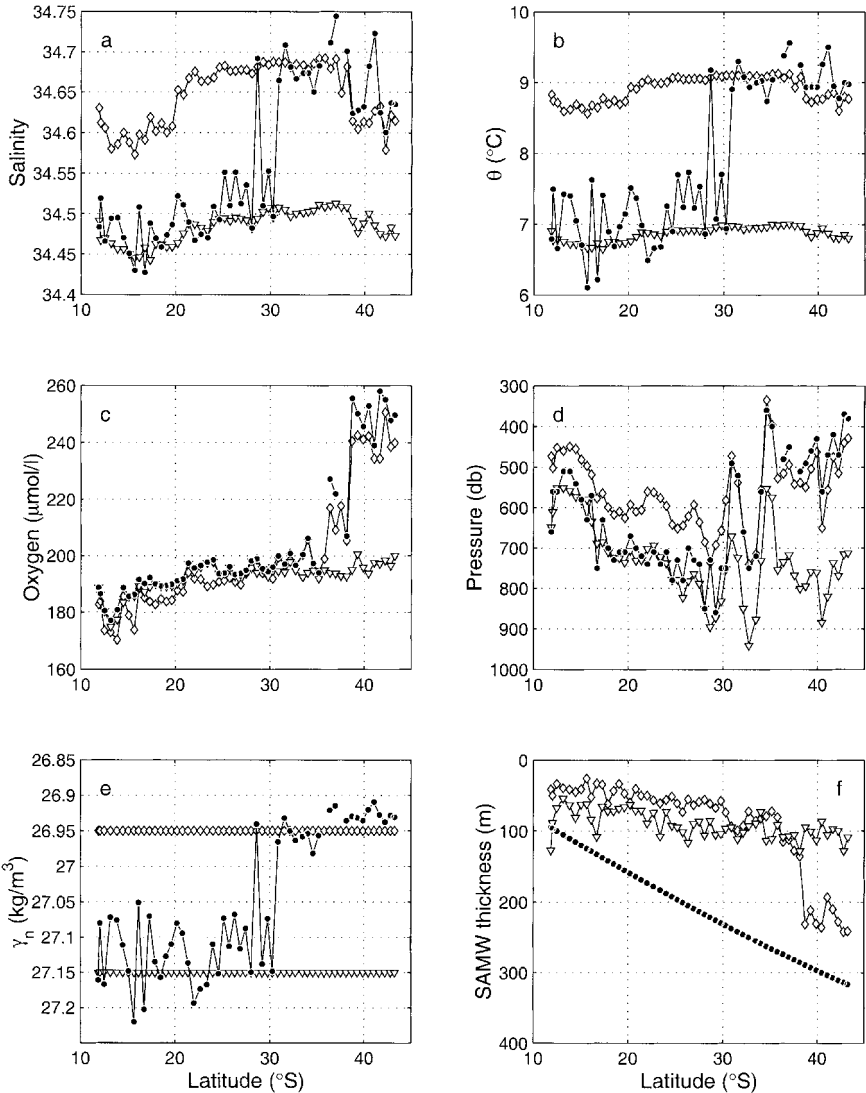
Figure 9. Properties of the Subantarctic Mode Water along P11. The oxygen maximum core layer is indicated with filled circles, the $\gamma_n = 26.95$ surface with diamonds, and the $\gamma_n = 27.15$ surface with open triangles. (a) salinity, (b) potential temperature, (c) oxygen, (d) pressure, (e) neutral density, (f) thickness of the density layer defined by 26.95 ± 0.05 (diamonds) and 27.15 ± 0.05 (triangles). In (f), the filled circles show the expected change in thickness due to the change in Coriolis parameter for a layer translated over the latitude range of the P11 section while conserving its planetary vorticity. The $\gamma_n = 27.15$ mode is approximately 320 m thick near 43S in the southeast Pacific.

oxygen maximum lies near the 26.95 surface south of 30S, and near the 27.15 surface north of 30S. South of 38S, oxygen on the 26.95 surface and the thickness of this layer increase dramatically, confirming the fact that SAMW entering the basin from the south is largely confined south of this latitude (Fig. 9c,f). Cold, fresh SAMW with density of about 27.15 enters from the east, and makes the dominant contribution to the oxygen maximum north of 30S. The initially high oxygen saturation of the southeast Pacific SAMW is reduced to 60–65% by the time it reaches P11 due to oxygen consumption and mixing along its transit of the subtropical gyre. Mixing has also eroded the strong pycnostad of the SAMW to some extent, although most of the change in thickness of the 27.15 mode can be accounted for by the change in latitude (i.e., Coriolis parameter) between the source region and the SEC (Fig. 9f). After the SEC bifurcates at 18S, part of the eastern SAMW flows cyclonically around the Gulf of PNG, where it forms an oxygen maximum at a depth of about 600 m in the NGCUC, and ultimately enters the Solomon Sea. The remainder of the SAMW carried westward in the SEC turns southward after the bifurcation and feeds the EAC. The increase in temperature and salinity of the southeast Pacific SAMW between the Coral and Tasman seas, and the nearly uniform properties on the 27.15 surface within the Tasman Sea, suggests that vigorous stirring by the eddy field rapidly homogenizes the temperature and salinity along isopycnals. Note that the thickness of the SAMW carried south in the EAC does not increase as rapidly as would be expected for a layer conserving its potential vorticity, another indication of active mixing there.

d. Antarctic Intermediate Water (AAIW)

A prominent salinity minimum between 700 and 1000 db on P11 marks the AAIW layer (Fig. 2b). The salinity minimum layer is thickest, lowest in salinity, and highest in oxygen at the southern end of P11, as expected for a water mass with a Southern Ocean source. Along 43S, the pattern of property extrema in the AAIW layer mirrors that of the SAMW above, suggesting inflow of "new" (i.e. low salinity, high oxygen) AAIW near station 71 at 154E, and outflow of "old" (i.e. high salinity, low oxygen) AAIW near the coast of Tasmania (inshore of station 78). Salinity minimum water with salinity <34.45 extends northward along 155E to 38S.

Even the AAIW of recent southern origin has fairly low oxygen concentrations (only 60% of saturation). Rather than an oxygen maximum, the AAIW is characterized by a layer of weak vertical oxygen gradient—an oxystad—between the high oxygen SAMW above and the oxygen minimum layer below. Rintoul and Bullister (1999) noted the low oxygen concentrations of AAIW south of Tasmania and suggested that the AAIW there was remote from a surface source, with the low salinity of the AAIW maintained by subsurface mixing across the SAF, consistent with the suggestion of Molinelli (1981).

A second salinity minimum is found at the northern end of P11, where AAIW enters the Coral Sea in the SEC (16–18 S) (Fig. 2b). The AAIW carried by the SEC is similar in salinity to, but warmer and lighter than, the AAIW entering from the south across 43S (Fig. 10). Part of the AAIW turns south in the EAC, where its salinity is increased by
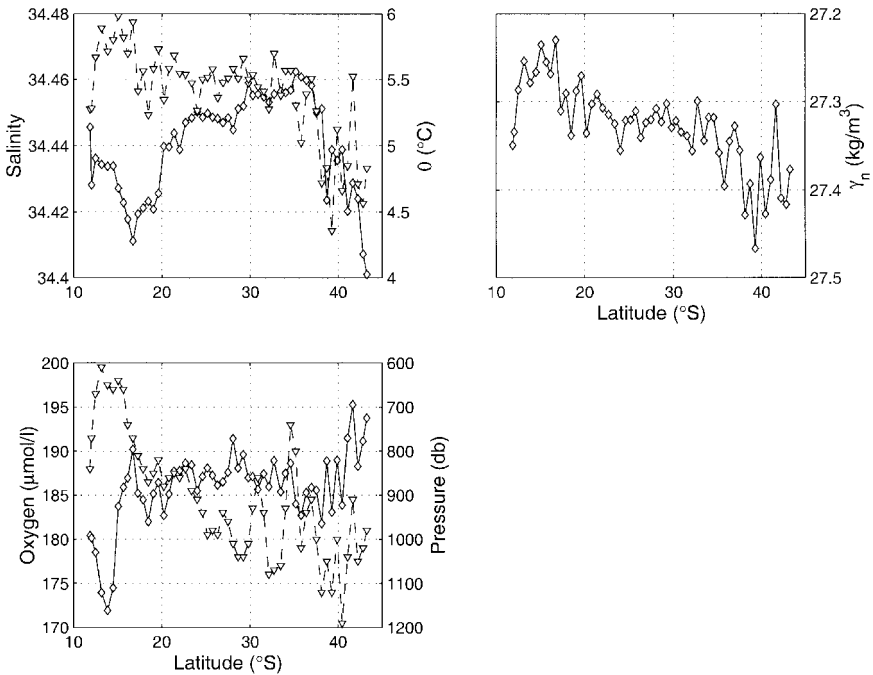
Figure 10. Salinity (diamonds), potential temperature, °C (circles), oxygen, μmol/l, (diamonds), pressure, db (circles) and neutral density (kg/m³) in the core layer of AAIW.

mixing before the EAC turns offshore and crosses P11 at 30S. Another inflow of AAIW across P11 is located at 28S, and is presumably caused by a branch of intermediate water entering the Tasman Sea directly from the east. This water is slightly higher in oxygen (192 μmol/l) and fresher (34.443) than the intermediate water carried by the EAC.

The presence of two varieties of AAIW with similar salinity, a cold variety entering from the south and a warm variety entering from the east, was noted by Wyrtki (1962a). He showed that AAIW entering from the east between New Zealand and Fiji split into two branches in the Tasman Sea, with some AAIW spreading directly west, and the remainder entering the Coral Sea between New Caledonia and Vanuatu. The 1985 *Franklin* survey also indicates that fresh intermediate water enters the Coral Sea between New Caledonia and Vanuatu.

Maps of properties on the core layer of the AAIW based on the SPAC data set help place the P11 data in a larger-scale context (Fig. 11). A strong salinity front along 15S (Fig. 11) marks the northern extent of the AAIW, between Vanuatu and the Solomon Islands. The AAIW entering from the east is formed in the southeastern Pacific. Although the pattern is not as obvious as at the SAMW level, the AAIW formed there is carried northwestward in two distinct branches: the northern branch carries AAIW around the subtropical gyre to enter the Coral/Tasman seas, while the southern branch carries AAIW westward near 35S. While the SAMW is blocked between New Zealand and Fiji by the eastward flow of the southern limb of the subtropical gyre, the AAIW is able to penetrate into the Tasman Sea at
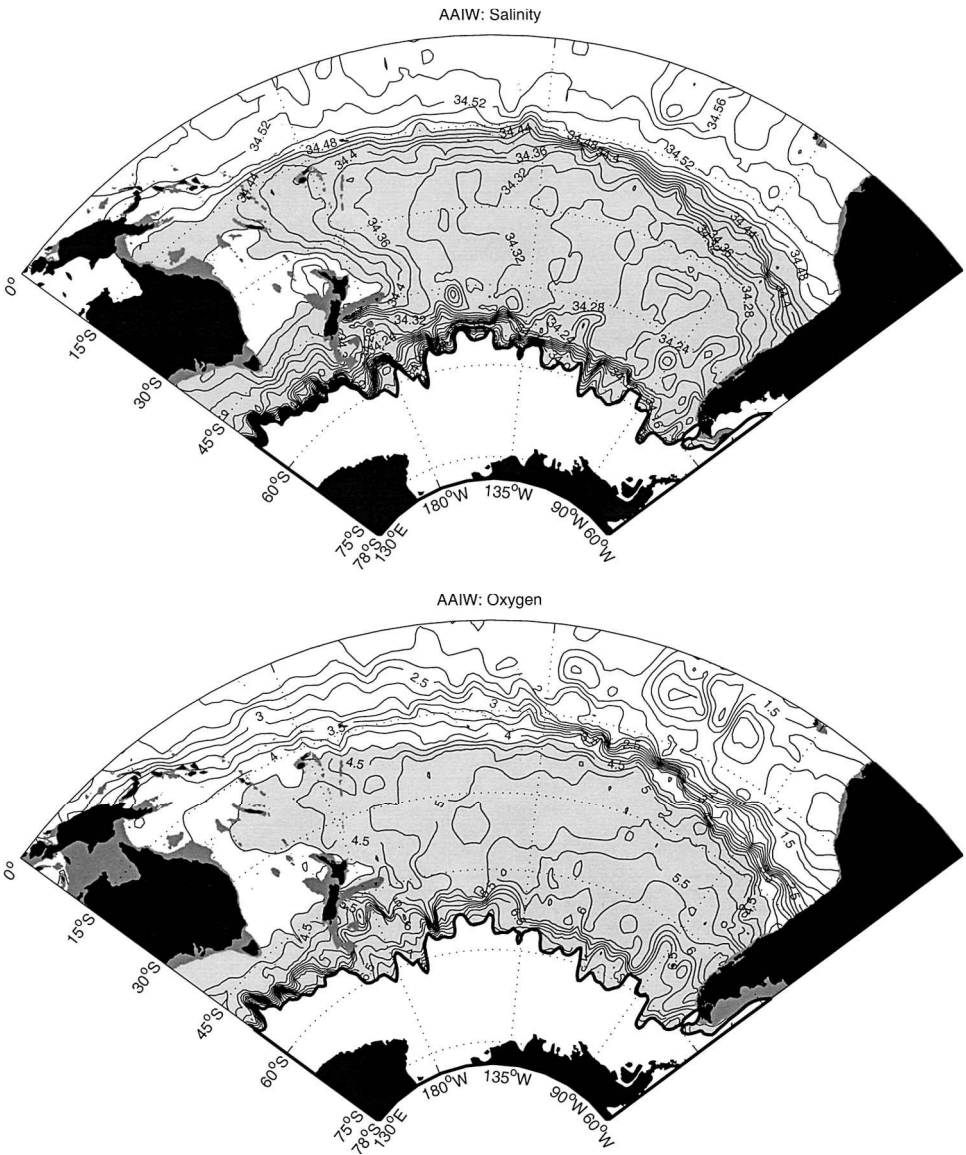
Figure 11. Water properties on the salinity minimum layer corresponding to the Antarctic Intermediate Water (AAIW). (a) salinity (shading indicates salinity lower than 34.46), (b) oxygen (ml/l) (shading indicates oxygen higher than 4.25 ml/l).

these latitudes due to the poleward shift of the subtropical gyre with depth (e.g. Morris *et al.,* 1996). The distribution of salinity and oxygen in the core layer of the AAIW shows that the intermediate water enters the Tasman Sea in a wide latitude band between 30S and 15S (Figs. 10, 11), as suggested by Wyrtki (1962a).

e. Oxygen minimum

A prominent oxygen minimum near 1500–2000 db is found along the entire P11 section. From north to south the oxygen minimum layer gets thinner and higher in oxygen. Note, for example, that the 170 μmol/l contours are separated by more than 2000 db at 14S and by 400 db at 43S (Fig. 2c). Oxygen concentrations at the minimum increase by about 30 μmol/l over the same latitude range. The prominent front at 16S in the salinity and oxygen anomaly plots, noted above in the discussion of thermocline water masses, extends to the depth of the oxygen minimum: north of 16S, the oxygen minimum is thicker and lower in oxygen. The lowest oxygen concentrations observed along the P11 section occur at stations 14 and 15, just offshore of the strong boundary current adjacent to PNG in the interior of the cyclonic Coral Sea gyre.

The distribution of properties on the oxygen minimum is broadly consistent with Wyrtki's (1961) inference of spreading from north to south within the Coral and Tasman seas. Along this path the oxygen minimum is eroded by mixing with higher oxygen water above and below this layer. However, the fact that water mass boundaries identified in the thermocline extend to the depth of the oxygen minimum suggests that the horizontal circulation at this level is sufficient to maintain these gradients in the presence of the lateral mixing, somewhat at odds with Wyrtki's assumption of minimal horizontal motion at the oxygen minimum.

f. Circumpolar Deep Water (CDW) and Bottom Water (BW)

The 43S portion of P11 shows a pool of cold ($<0.7°C$) water banked up against the continental slope of Tasmania, a signature of the weak deep western boundary current carrying water of recent southern origin into the southern Tasman Sea (Fig. 2a). Reid (1986) had inferred the presence of such a boundary current from tracer distributions in the Tasman Sea.

Toward the north along P11, the BW becomes warmer and saltier due to mixing with the CDW above, while the CDW gets fresher and cooler (Fig. 12). At the southern end of P11 (station 69) the core of the CDW is found at 2820 db with a salinity of 34.728 and a potential temperature of 1.52°C (Fig. 12c). Below this maximum the potential temperature and salinity decrease with depth reaching values less than 0.64°C and 34.705 at the bottom. At station 37, just south of the trough connecting the East Australian and Coral Sea Basins, the CDW is 0.1°C cooler and 0.006 fresher, while the BW is about 0.17°C warmer and 0.008 saltier than at station 69. (Warren (1973) surprisingly found *higher* salinities in the CDW at 28S than at 43S, which led him to conclude the salinity maximum water entering from the south must vary in time. The P11 data, in contrast, show a relatively steady decrease in salinity to the north in the salinity maximum layer, consistent with erosion by vertical mixing.)

Farther north, in the channel connecting the Tasman and Coral seas, the salinity maximum water mixes with AAIW above and warms and freshens. The BW is too dense to enter the Coral Sea, and the deep salinity maximum extends to the sea floor there. At station
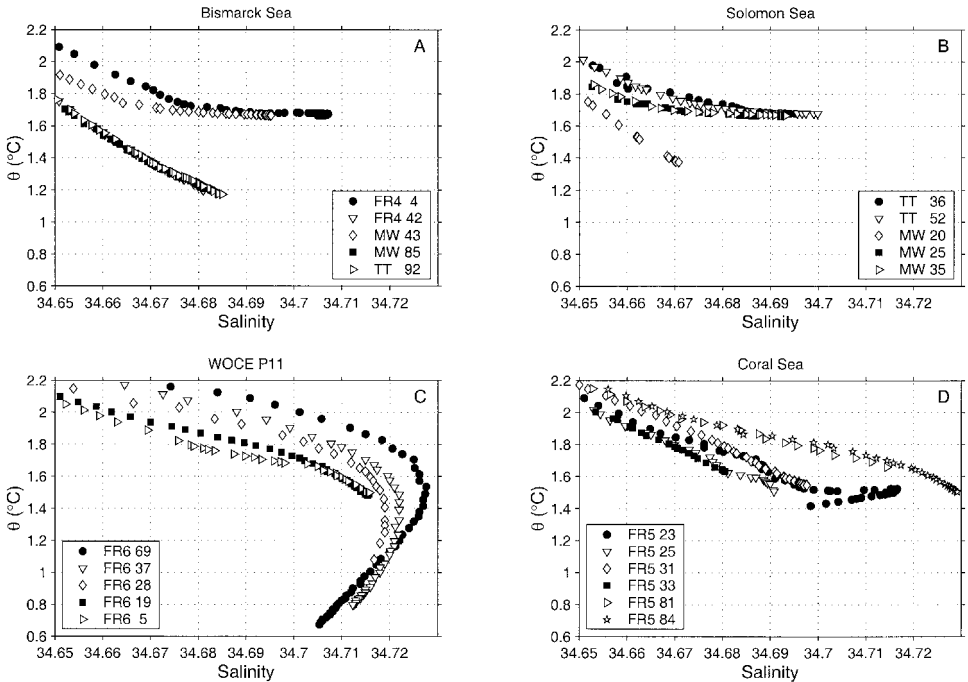
Figure 12. Expanded view of the portion of the potential temperature—salinity relationship corresponding to deep and bottom water. Position of the stations is shown in Figures 1 and 13. The 4 panels are laid out so as to roughly correspond to their geographical positions: (a) stations in the northwest quadrant (Bismarck Sea, East Caroline/Mariana Basin); (b) northeast quadrant (northern Solomon Sea, Vitiaz Strait, St Georges Channel); (c) P11 stations; (d) southeast quadrant (southern Solomon Sea, eastern and central Coral Sea). Cruise abbreviations: FR4—*Franklin 8504;* FR5—*Franklin 8505;* FR6—*Franklin 9306;* MW—*Moana Wave 8601;* TT—*Thomas G. Thompson 8506.*

19, in the deep basin of the Coral Sea, the potential temperature is 1.46°C, identical to the coldest potential temperature found by Wyrtki (1961) in this basin.

The evolution of the Θ-S curves through the Tasman Sea, and the fact that waters above the CDW core are much cooler at the north of the East Australian Basin than at the south, show that diapycnal mixing of heat and salt dominate over isopycnal advection in determining the Θ-S properties of the deep water in this basin. Warren (1973) reached a similar conclusion based on a one-dimensional advective-diffusive balance for temperature. High rates of vertical mixing in deep boundary currents have been inferred by other investigators (e.g. Roemmich *et al.* (1996) in the Samoan Passage).

Wyrtki (1961) first described the circulation of deep and bottom water in the Tasman/Coral seas. He proposed that the bottom waters of the Coral Sea and the Solomon Sea basins both came from the East Australian Basin, while the bottom waters in the New Hebrides Basin, the New Caledonia Trough, and the Fiji Basin came from the Central
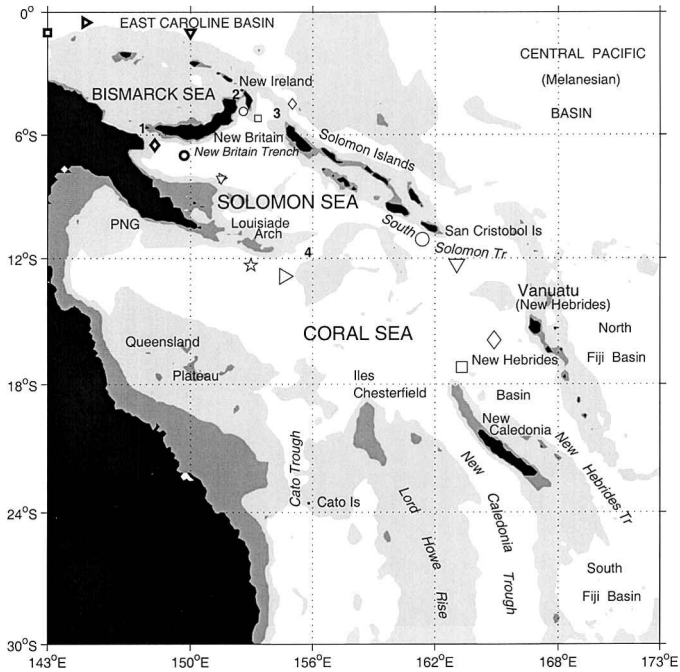
Figure 13. Position of the stations shown in Figure 12. Stations presented in Figure 12 in panel (a) are shown by bold symbols; in panel (b) by normal symbols; in panel (c) by the symbols in Figure 1; and panel (d) by large symbols. Light shading indicates depth shallower than 2500 m; dark shading indicates depth shallower than 250 m. Narrow passages and straits are indicated with numbers: 1—Vitiaz Strait; 2—St. Georges Channel; 3—Solomon Strait; 4—Pocklington Trough.

Pacific Basin (see Fig. 13 for a detailed map of the bathymetry). Lindstrom and Hayes (1989), in contrast, found that the deep layers of the southern Solomon Sea Basin are supplied from the east, by water entering the basin through the South Solomon Trench. However they noted that more observations were required to determine the source of the deep waters in the northern Solomon Sea Basin.

To investigate the source of the deep waters in the Coral and Solomon seas we compare deep high-resolution CTD measurements from a number of recent cruises (Figs. 12, 13). The deep waters in the Solomon Sea (Fig. 12a,b) are horizontally homogeneous throughout the basin, and the Θ-S curves found for the New Britain Trench and near the northern entrance to the Solomon Sea at the Vitiaz Strait, St. Georges Channel and the Solomon Strait are similar to those found in the South Solomon Trench (Fig. 12d). This indicates that the deep waters in the Solomon Sea primarily enter from the east. The CDW entering from the east is cooler and fresher, and the salinity maximum core is deeper, than water entering the Coral Sea from the East Australian Basin. Small horizontal gradients in temperature and salinity in the deep layers within the Coral and Solomon seas, and sharp differences between water properties there and the East Caroline Basin, indicate that the inflow of deep

water to the Solomon Sea from the north through the Vitiaz Strait and St. Georges Channel is very limited.

The East Caroline Basin Deep Water (referred to as the North Pacific Deep Water (NPDW) by Johnson and Toole (1993)) found to the north of the islands bounding the Solomon Sea is even fresher and cooler than the deep water which enters the Solomon Sea from the east (Fig. 12a). This is an indication that the deep and bottom waters found in the Solomon Sea and in the eastern part of the Coral Sea are derived from the CDW (or Lower Circumpolar Water (LCPW), Johnson and Toole, 1993) spreading north from the ACC as a deep western boundary current along the Tonga-Kermadec Ridge, through the Samoa Passage, and finally across the equator to the North Pacific (for details see e.g., Reid, 1986; Taft *et al.,* 1991; Johnson and Toole, 1993). While the densest water in the boundary current is prevented from spreading to the west by topography, lighter CDW spreads west toward the East Mariana Basin, and also supplies deep water to the eastern Coral Sea and the Solomon Sea.

The distribution of silica in the South Pacific also supports this view. CDW entering the Pacific from the Southern Ocean is initially low in silica (<90 µmol/l, see e.g. Schmitz, 1996), while NPDW can have values as high as 180 µmol/l. As CDW spreads north the silica content increases to 120 µmol/l at 32S (Toole *et al.,* 1994), and to 126 µmol/l at the Samoan Passage (Roemmich *et al.,* 1996). Lindstrom and Hayes (1989) found silica concentrations of about 135 µmol/l in the South Solomon Trench at depths below 3500 m, and values less than 110 µmol/l in the central Coral Sea Basin. The low silica in the Coral Sea Basin is an indicator of the ''southern'' source of deep water supplied from the East Australian Basin, while the higher values in the eastern part of the Coral Sea reflect deep water inflow derived from the "eastern" source.

5. The circulation

Several attempts have been made to quantify the circulation and obtain mass balance in this region (e.g. Scully-Power, 1973; Thompson and Veronis, 1980; Andrews and Clegg, 1989). The most comprehensive recent study is that of Ridgway and Godfrey (1994), who used all available historical data to estimate the circulation above 2000 m in a box enclosing the Tasman Sea and the southern part of the Coral Sea. However, most previous hydrographic stations occupied in the Tasman/Coral seas have been shallow, the data sets have been combined from various cruises over a number of years (and so are usually smoothed in space), and/or the measurements have been too sparse along the cruise tracks to resolve the details of circulation in the region. The P11 section closes off the western part of the subtropical gyre of the South Pacific, and is particularly well suited to determine the zonal flows into and away from the western boundary.

a. Choice of reference level

As noted in Section 2, most studies of the circulation of the Coral and Tasman seas have assumed a level of no motion at mid-depth. However, the vertical shear associated with the

strong flows in this region extend to near the sea floor, and sparse direct velocity measurements suggest that, at least for the EAC and eddies spawned from the EAC, the currents extend very deep in the water column. In addition, the water mass properties described above are consistent with a deep reference level.

To gauge the sensitivity of the transport results to the choice of reference level, transports relative to zero velocity surfaces at 1300 db, 2000 db and the deepest common depth were compared. Integrating the geostrophic velocity relative to the deepest common depth along the nearly-enclosed box defined by P11 results in a net inflow to the region of 3.6 Sv. Noting that the sum of the absolute value of the station pair transports across the boundaries of the box is more than 500 Sv, the estimated imbalance is small. Including the Ekman transport (calculated from the July monthly mean surface wind stress of Hellerman and Rosenstein, 1983), which is positive (directed into the region) across all boundaries, the resulting imbalance is about 8.7 Sv.

The integrated geostrophic transport across the section relative to 2000 and 1300 db does not conserve mass, resulting in a net discrepancy of 18.1 (23.2 including Ekman) and 1.1 Sv (6.2 including Ekman), respectively. While the net imbalance is small in the 1300 db case, the small imbalance results from a net inflow of 12.5 Sv (17.6 including Ekman) above 1300 db, and a net outflow of 11.4 Sv below this level. A conversion of this volume of upper and intermediate water to deep water is inconsistent with both the observed water properties and air-sea fluxes in this region. In contrast, a reference level near the bottom results in a more consistent circulation pattern, both in terms of net transport and the transport of individual layers, as described below.

An attempt was made to use currents measured by the ADCP to reference the geostrophic velocities. Transports referenced to the ADCP velocities result in a net outflow of 25 Sv in the upper 250 m alone: this large imbalance likely reflects the impact of biases in the ADCP velocities introduced by the ship's gyro compass, and the ADCP was rejected as a reference for the transport calculations. In the following, transport relative to the deepest common depth is presented as our best estimate of the circulation. (A uniform reference level velocity of less than 1 mm/s is sufficient to achieve mass balance, but results in negligible changes to the transports of individual currents discussed below.) Transports relative to 1300 and 2000 db are included for comparison with earlier studies.

b. The geostrophic circulation

The cumulative transport integrated from north to south along P11 provides an overview of the major circulation features of the southwest Pacific (Fig. 14). The SEC carries about 55 Sv into the Coral Sea between 14S and 19S. The NGCUC/NGCSC returns 26 Sv to the east, while the remainder turns south to feed the EAC. The cumulative transport rises and falls to the south through the Tasman Sea as the section crosses a number of recirculating flows or eddies. Although the P11 section alone does not allow us to determine the zonal scale of these currents, similar features have been noted by earlier investigators (e.g. the dynamic topography maps of Hamon, 1965; 1970), and they may be relatively permanent
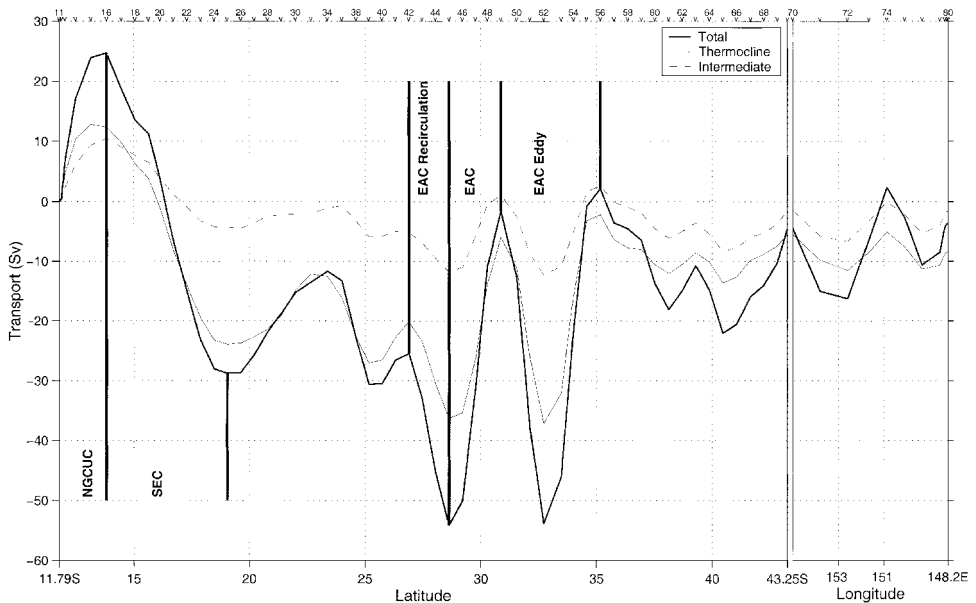
Figure 14. Cumulative transport (Sv) integrated from north to south along P11. Flow toward the east and north is positive.

features rather than transient eddies. The EAC leaves the coast and crosses P11 near 30S, with more than half of the 55 Sv returning to the west in a tight recirculation between 27S and 29S. The transport of the EAC warm core eddy (60 Sv) is approximately equal to that of the EAC itself. The transport along the southern end of P11 is relatively weak and oscillates in sign. In the rest of this section, we examine these flow features in more detail.

i. The Coral Sea circulation. The circulation across P11 is broadly consistent with previous maps of the circulation in this region, but the fine spatial resolution of this synoptic section reveals additional details of the inflow to the Coral Sea. The velocity section (Fig. 15) reveals three distinct high velocity cores in the broad band of westward flow associated with the SEC. The northern branch, between 15°30′S and 13S, is the weakest of the three and carries 14 Sv into the Coral Sea. A strong water property front at 16S separates the northern and middle branches, with warmer, saltier and lower oxygen water found north of the front. The middle branch is the strongest of the three, with maximum surface speeds of 50 cm/s and a net transport relative to the bottom of 24 Sv between 16S and 17S. The southern branch, between 17S and 18S, carries 17 Sv of water with properties similar to that found in the middle branch. Based on the property distributions discussed above, we infer that the northern branch of the SEC is supplied by water entering the region between Vanuatu and the Solomon Islands, and the southern two branches are fed by inflow between Vanuatu and New Caledonia.
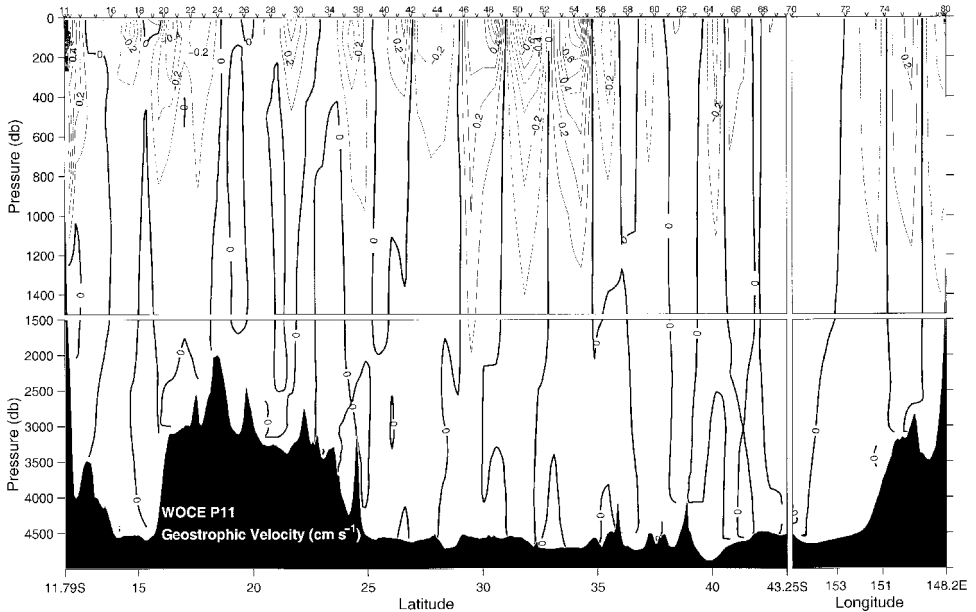
Figure 15. Geostrophic velocity (relative to the deepest common depth; cm/s) across WOCE section P11. Dashed contours indicate westward and southward flows.

The total geostrophic transport of the SEC is 55 Sv relative to the bottom (Fig. 16a). Estimates of SEC transport obtained in earlier studies are summarized in Table 1. Accounting for the differences in reference levels used and in the region over which the transport estimates are integrated, these estimates are remarkably similar. Further upstream in the central Pacific, the transport of the SEC is concentrated in the upper thermocline, with a transport of 30–36 Sv in the upper 400 m south of 2.5S (Kessler and Taft, 1987; Taft and Kessler, 1991; Picaut and Tournier, 1991; Donguy and Meyers, 1996). The SEC deepens to the west, so that a substantial part of the flow is below 400 m when the current reaches P11. Our transports are also broadly consistent with recent estimates of the strength of the subtropical gyre as a whole: for example, McCartney and Baringer (1993) found a top-to-bottom northward transport of 60 Sv across 32S east of the Kermadec Ridge, with 35–42 Sv above 2000 m, while Godfrey (1989) estimated a Sverdrup circulation of 40 Sv east of the date line at 30S.

As described in Section 2, the SEC bifurcates at 18S near the coast of Australia, with the southern branch forming the EAC, and the northern branch re-circulating in the Gulf of Papua New Guinea. At the northern end of P11, the subsurface flow of the NGCUC with current speeds as high as 55 cm/s is supplemented by the New Guinea Coastal Surface Current (NGCSC; Fine *et al.,* 1994) which flows in the same direction with velocities up to 75 cm/s. A very narrow westward flowing counter-current is found adjacent to the coast. The net eastward transport of the combined NGCUC/NGCSC is 26 Sv (Fig. 16a), close to

estimates based on earlier RV *Franklin* cruises in 1985 (27 Sv) and in 1990 (33 Sv, Burrage, 1993).

Water supplied by the NGCUC ultimately leaves the Solomon Sea through Vitiaz Strait and St. Georges Channel (Lindstrom *et al.,* 1990; Tsuchiya *et al.,* 1989; Butt and Lindstrom, 1994). Direct measurements in Vitiaz Strait show a mean equatorward transport of 15.8 Sv (Murray *et al.,* 1995), and a range of 10 to 20 Sv. Butt and Lindstrom (1994) show that St. Georges Channel likely carries about 8 Sv. The combined transport of 24 Sv is close to our estimate based on the P11 section. The NGCUC transport across P11 is also consistent with the Sverdrup calculation of Godfrey (1989), who shows that 23 Sv of equatorward transport via the western boundary current is implied by Sverdrup balance. Our estimates, however, do not include flow which enters the Solomon Sea directly from the SEC, without crossing P11. Andrews and Clegg (1989) estimate this branch carries an additional 8 Sv in the upper 1000 db.

ii. Circulation in density layers in the Coral Sea. About 2 Sv of TSW is carried into the Coral Sea in the northern branch of the SEC across P11 (Fig. 16b). Some TSW in this region is formed in the northern Coral Sea, and some enters the Coral Sea from one of the major areas of TSW formation east of the Solomon Islands. A low-salinity tongue spreading southward east of the Solomon Islands and entering the Coral Sea is shown clearly in Figure 3. Most of the TSW circulates cyclonically in the Gulf of PNG, and 1.5 Sv is returned to the east in the NGCSC.

As discussed in Section 4, SLW with lower oxygen content enters the Coral Sea between the Solomon Islands and Vanuatu, and the high-oxygen southern branch is fed by inflow between Vanuatu and New Caledonia (Fig. 16c). The transport of northern SLW ($\gamma_n = 23.6$ to 25.6) into the Coral Sea is 19.2 Sv, of which 3.3 Sv is carried by the northern branch of the SEC. The water carried by the northern branch continues across the Coral Sea and supplies the GBRUC and NGCUC. The outflow of SLW in this layer across P11 in the NGCUC (3.3 Sv) matches the inflow to the Coral Sea carried by the northern branch of the SEC (Fig. 16c). The total net inflow of SLW into the Coral Sea in the neutral density layer between 23.6 and 26.8 is 32 Sv, with 10.1 Sv (5.6 Sv from the northern branch and 4.5 Sv from the high-oxygen branch) circulating around the Gulf of PNG and entering the Solomon Sea in the NGCUC. The remainder of the SLW turns south to feed the EAC.

The transport of SAMW and AAIW entering the Coral Sea across P11 is 18.7 Sv, with 3.9 Sv transported in the northern branch of the SEC north of 16S (Fig. 16d,e). The NGCUC carries 12.5 Sv of SAMW and AAIW across P11. The SAMW and AAIW enter the Tasman/Coral Sea farther south than the SLW, as a result of the poleward shift with depth of the northern arm of the subtropical gyre evident in the dynamic topography (Fig. 17).

The circulation of CDW and BW across P11 is relatively weak (Fig. 16f). About 6 Sv of deep and bottom water re-circulate in the Coral Sea across P11. 3 Sv of CDW flowing from the East Australian Basin supplies the deep layers of the Coral Sea. This inflow runs almost
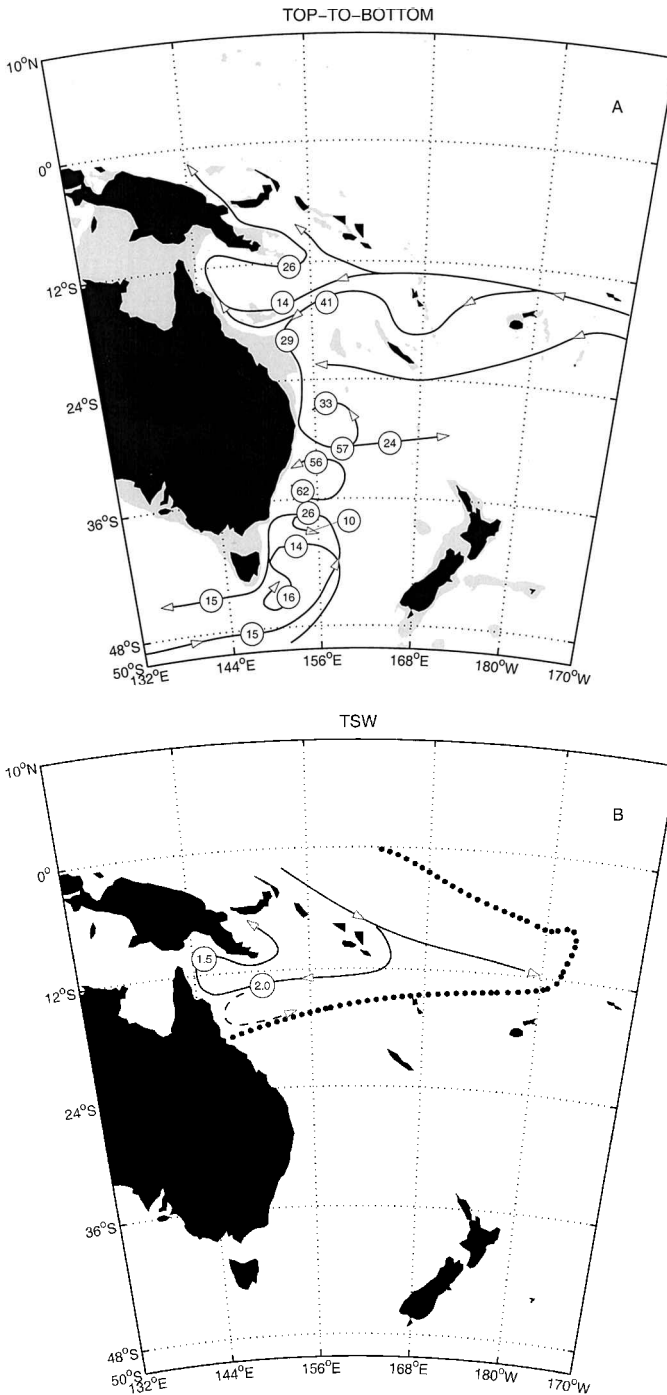
Figure 16. Circulation summary of the western part of the South Pacific. Paths of water masses are shown by solid lines with arrows, and transports are indicated in circles (Sv). (a) total. (b) TSW. (c) SLW; paths of the southern component of SLW are shown by dashed lines and transports are shown in squares. (d) SAMW. (e) AAIW. (f) CDW and BW; paths of CDW are shown by solid lines; paths of BW are shown by dashed lines.
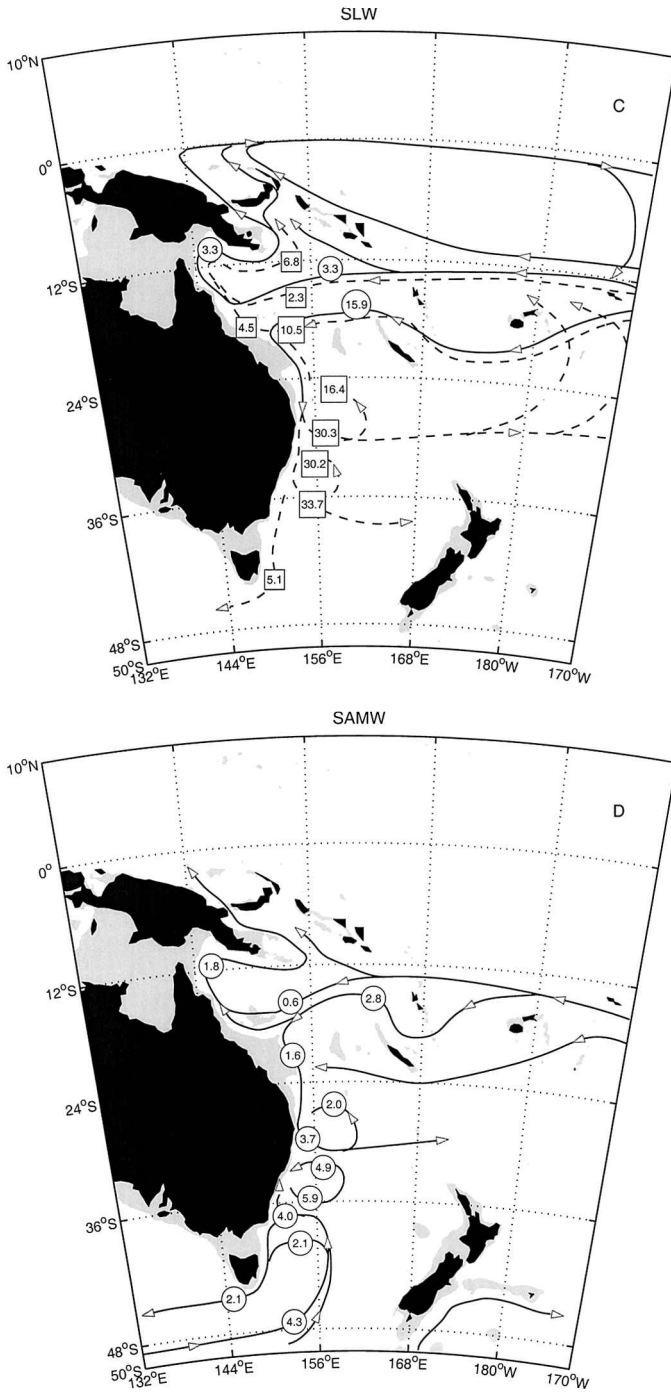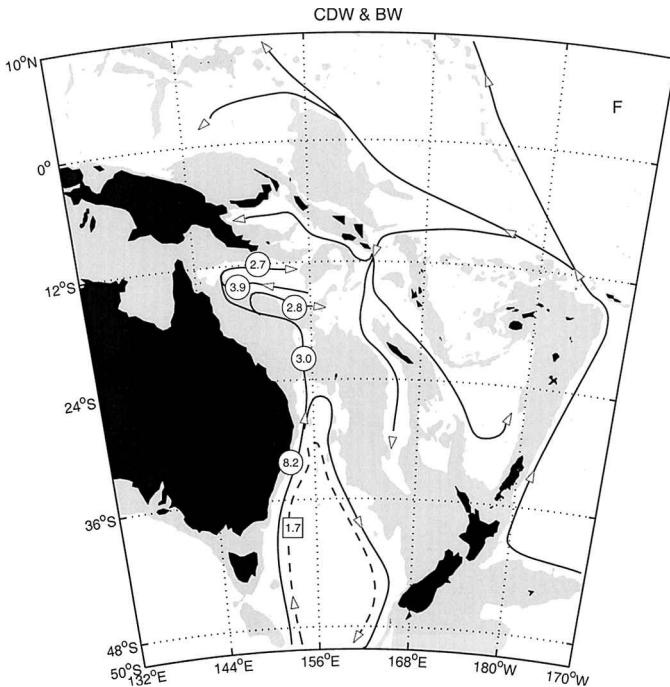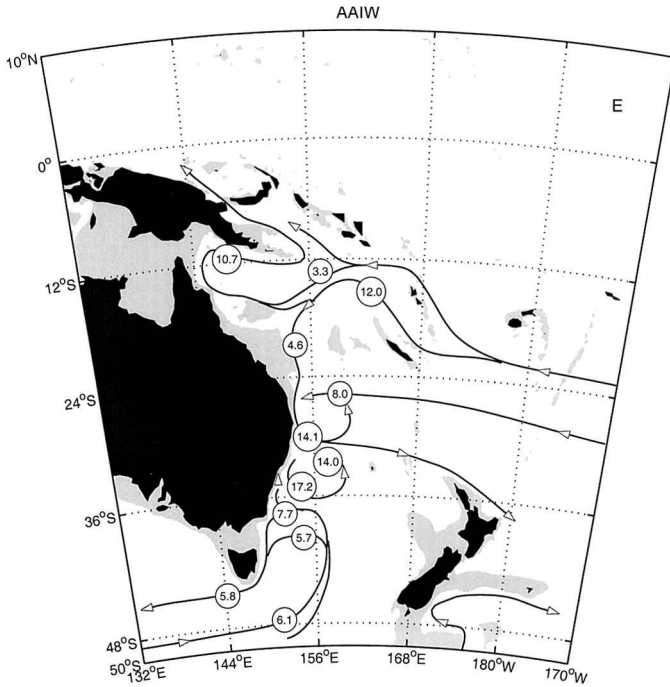
Figure 16. (Continued)

Figure 16. (Continued)

Table 1. Estimates of the transport of the South Equatorial Current.

Region	Layer/Ref. level	Transport (Sv)	Source
27S-Solomon Islands	0–1750/1750	48	Wyrtki (1962b)
north of 20S (across 157E)	0–1500/1500	37	Scully-Power (1973)
Vanuatu-Solomon Islands	0–1000/bottom (adjusted)	24	Andrews and Clegg (1989)
P11	0–bottom/bottom	56	
	0–2000/2000	54	
	0–1300/1300	36	

parallel to P11, crossing it between stations 29 and 31 and once again between stations 20 and 23, and so is not well resolved by this section. The northern branch of the SEC also delivers about 3.9 Sv of deep water from the east. The inflow of deep water from the south and east is roughly compensated by 2.7 Sv flowing east beneath the NGCUC, and by 2.8 Sv of eastward flow between the northern and middle branches of the SEC.

iii. The circulation field of the EAC. We have shown that 26 Sv of the 55 Sv carried into the Coral Sea by the SEC exits the Coral Sea in the NGCUC. The remainder, 29 Sv, flows south from the SEC bifurcation at 18S to feed the EAC (assuming zero net transport through Torres Strait).

Along the Australian coast the EAC forms a system of deep eddies reaching at least 2000 m depth with the main flow located along the continental slope. The uniformity of water mass characteristics along isopycnals south of Cato I. between 24 and 28S (Fig. 5) indicates that the current is continuous along the western boundary of the Tasman Sea (Rochford, 1968), and that vigorous stirring by EAC eddies and meanders acts to homogenize water properties.

The EAC separates from the coast and crosses P11 near 30S. The steeply sloping isopycnals associated with the current persist from the surface to the bottom (Fig. 2d). The total geostrophic transport of the EAC after separation is 56.6 Sv. The EAC transport and the total/upper 1300 m geostrophic transport ratio are consistent with results obtained earlier (Boland and Hamon, 1970; Hamon, 1970; Mulhearn *et al.,* 1988).

After separating from the coast, one branch of the EAC recirculates to the north and then west, crossing P11 again at 28S, while the remainder can be traced as a continuous meandering eastward jet across the Tasman Sea and lying at about 25–30S between New Zealand and Fiji (Fig. 16a). Our transport estimate of 13.7 Sv in the Tasman Front in the upper 500 m (relative to the bottom) is close to values found in earlier studies (e.g. Stanton, 1981; Morris *et al.,* 1996). Of the top-to-bottom transport of 57 Sv where the EAC leaves the coast, 33 Sv recirculates to the west, leaving a net outflow of 24 Sv. Other evidence of a tight recirculation in the Tasman Basin can be seen on maps of sea-surface temperature, tracer distributions in the Tasman Sea (Fig. 6), and in the maps of earlier investigators (e.g. Hamon, 1965, 1970; Ridgway and Godfrey, 1994).

A warm-core anticyclonic eddy is located south of the latitude where the EAC turns
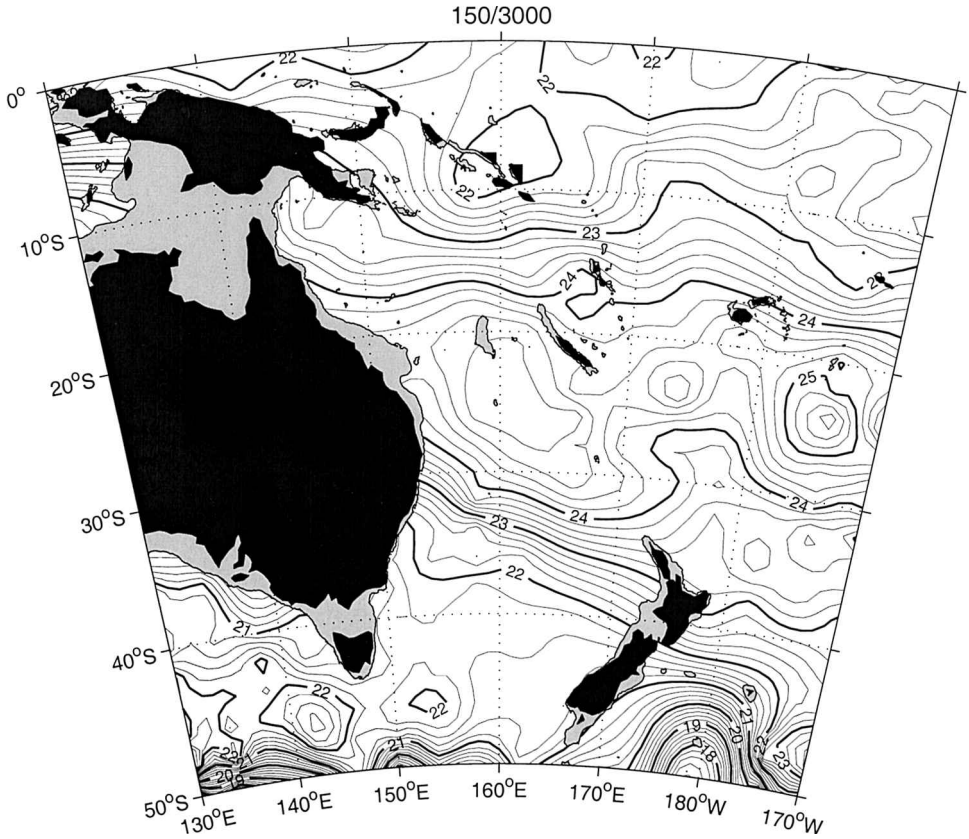
Figure 17. All geopotential anomaly maps are based on the individual station data set of Gouretski and Jancke (1996), which have been averaged on a 4° longitude × 2° latitude grid in neutral density layers. Depths less than shown surface are shaded. (a) Dynamic height (J/kg) at 150 db relative to 3000 db. (b) Dynamic height (J/kg) at 500 db relative to 3000 db.

offshore (Fig. 2). A detailed review and analysis of the formation and evolution of EAC anticyclonic eddies can be found in Nilsson and Cresswell (1981). The total transport of the eddy is 60 Sv, slightly in excess of the EAC transport. Like the EAC, the eddy extends from the surface to the sea floor, and at a depth of 1300 m the geostrophic velocities exceed 10 cm/s.

Transport in density layers shows that the EAC after separation from the coast transports about 30.3 Sv of SLW and 17.7 Sv of significantly modified intermediate water (the SAMW and the AAIW; Fig. 16d,e). The AAIW transported by the EAC is higher in salinity (34.45) and lower in oxygen (188 μmol/l) than intermediate waters entering the Coral Sea from the east (34.41 and 190 μmol/l, respectively), and the Tasman Sea from the south (34.40 and 195 μmol/l, Fig. 10). The high salinity and low oxygen of the AAIW in the
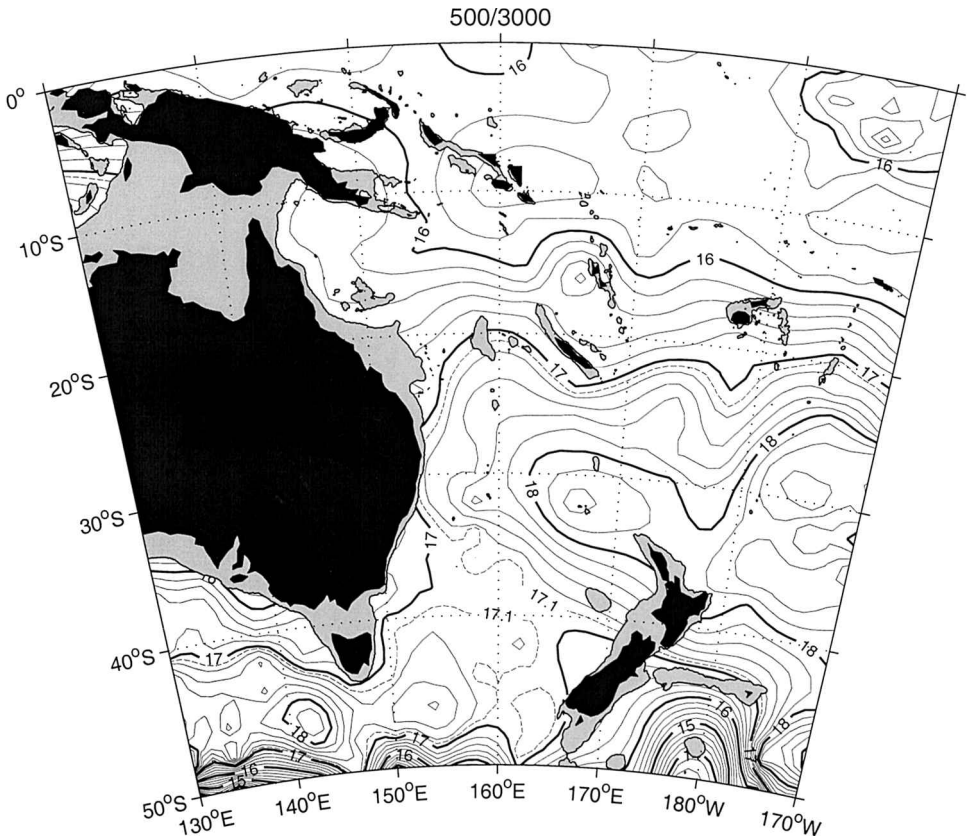
500/3000

Figure 17. (Continued)

central Tasman Sea reflect a relatively long residence time and strong mixing in the recirculation gyre of the EAC.

The main inflow of the deep and bottom waters from the south toward the Cato I. Trough crosses the P11 section between 28 and 24S (Fig. 16f). The total transport of the CDW and bottom waters carried by this deep flow is 8.2 Sv and 1.7 Sv, respectively. About 3 Sv of CDW passes through the Cato I. Trough and enters the Coral Sea, while the remainder returns to the south in the eastern Tasman Sea.

iv. The circulation of the southern Tasman Sea. The circulation of the southern Tasman Sea is characterized by highly variable flows and a lack of strong mean currents. The maps by Wyrtki (1962b) and Reid (1986) show that part of the EAC continues beyond the separation point as far south as Tasmania. Previous studies disagree as to whether this flow turns east (e.g. Wyrtki, 1962b; Stramma *et al.,* 1995) or west (e.g. Reid, 1986) on reaching the southern tip of Tasmania. Estimates of the net flow through the Tasman Sea between

Tasmania and New Zealand also vary (see Section 2), although the consensus appears to be that there is a net flow to the south.

The flow at the southern end of P11 agrees well with the circulation patterns inferred from the water property distributions. Near the coast of Tasmania, a band of southward flow carries 15.3 Sv of modified subtropical water across 43S. The strongest inflow of water from the south occurs between 154E and 155E, where the thickest SAMW and freshest AAIW is found (Fig. 2). This current branch crosses the 43S section then turns east to cross P11 between 40S and 42S. The total transport of this current is 14.5 Sv across 43S, including 4.3 Sv of SAMW and 6.1 Sv of AAIW, and 19.8 Sv across 155E (Fig. 16).

After crossing the southeast corner of the box defined by P11, this flow turns north and west to intersect the P11 section again at 37.5S and 40S (along with additional inflow across 43S east of 155E), where two strong westward flows carry high oxygen subantarctic mode waters across P11 (Fig. 2). These currents are presumably part of the anticyclonic cell apparent in the dynamic topography (Fig. 17), and transport about 8.2 Sv of SAMW and 16.4 Sv of AAIW to the west (Fig. 16). The lower oxygen concentrations in the SAMW carried by the westward flow located at 37.5S (210–240 μmol/l) compared with that at 40S (235–250 μmol/l) is indicative of some entertainment and lateral mixing with the waters which occupy the central part of the Tasman Sea. The total westward transports delivered by those flows are 25.8 Sv and 14.3 Sv respectively, with 10.1 Sv recirculating eastward at 38.5S due to eddies.

The dynamic topography maps (Fig. 17) support Reid's suggestion that the southern extension of the EAC turns to the west on reaching the southern tip of Tasmania. The repeat WOCE SR3 section between Tasmania and Antarctica provides the best observations of the westward flow south of Tasmania. The mean net transport of the "Tasman outflow" based on 6 CTD sections occupied between 1991 and 1996 is 8 Sv (Rintoul and Sokolov, 2000). The westward flow occupies most of the water column, and is part of the westward limb of the anticyclonic circulation evident in the dynamic topography near 45S. The eastward flow at the southern periphery of the anticyclonic cell is found south of 47.5S.

The net transport across P11 south of 30S, where the EAC leaves the coast and crosses the section, is close to zero. About 10.5 Sv of subsurface and intermediate waters from the subantarctic zone enter the region at the southern periphery of the anticyclonic cell, but most of this is returned to the south so that little SAMW and AAIW entering across 43S continues northward through the Tasman Sea, consistent with the property distributions described in Section 3. Smaller-scale recirculations along 43S increase the total volume of water carried across the section by a factor of 2.

An occupation of the 43S section several months earlier in April–May 1993 (Rosenberg *et al.,* 1995) supports these conclusions. Southward flow of subtropical water near the Tasmanian coast was supplemented by southward flow of modified subantarctic water farther offshore. Even farther offshore, "new" SAMW and AAIW was carried into the Tasman Sea by the anticyclonic gyre, which appeared to be shifted to the east in April–May.

6. Discussion: Intermediate waters and interbasin exchange

Several authors have described the low latitude western Pacific as a ''water mass cross-roads'' where intergyre and interbasin exchange is enhanced (Fine *et al.,* 1994; Lukas *et al.,* 1996; Tsuchiya *et al.,* 1989; Schmitz, 1996). In particular, water from the South Pacific which ultimately feeds the Equatorial Undercurrent, the Indonesian Throughflow, and the North Pacific, must first pass through the Coral and Solomon seas to reach the equator. However, questions remain as to how much water is carried from the South Pacific to the equator, and in what density range.

Our results confirm the continuity of a coastal undercurrent south of PNG, linking the GBRUC and the NGCUC flowing through Vitiaz Strait on the northern side of PNG. The total eastward flow is 26 Sv. Approximately half of this is realtively high oxygen water which enters the Coral Sea in the middle branch of the SEC near 16S. The remainder is low oxygen water carried into the Coral Sea in the northern branch of the SEC. The low oxygen thermocline water is part of a tropical gyre consisting of eastward flow along the equator in the EUC, southward flow in the central Pacific, westward flow in the northern branch of the SEC, and closed by equatorward flow in the low latitude western boundary current formed by the GBRUC/NGCUC. The higher oxygen thermocline and intermediate water in the core of the NGCUC on P11 is supplied by the subtropical gyre via the middle branch of the SEC.

Schmitz (1996) has discussed the NGCUC in the context of the global thermohaline circulation. He suggested that mode water and intermediate water must enter the Pacific from the south to balance the export of water through the Indonesian passages. Following modification in the South Pacific, this inflow passes through Vitiaz Strait and St Georges Channel to feed the equatorial and North Pacific (where additional water mass modification occurs before the water flows out of the Pacific through the Indonesian passages). Schmitz compared estimates of the transport in several layers across 32S (based on the results of Toole *et al.,* 1994) and through Vitiaz Strait (based on the results of Murray *et al.,* 1995) and found that the flow leaving the basin was dominated by thermocline water, while the flow entering from the south was dominated by denser mode and intermediate water. He hypothesized that the required conversion of dense to light water occurred in the Peru Current, although he did not have a lot of data to confirm this.

Our estimates of transport in the NGCUC south of PNG suggest that relatively little diapycnal conversion is required between 32S and the northern Coral Sea. Wijffels *et al.* (2000) recently presented the revised geostrophic transport across WOCE section P6 constrained by ALACE float measurements of velocity at 900 m. They showed that 17.2 Sv of thermocline water with neutral density γ_n between 25.0 and 27.0 and 15.7 Sv of intermediate water ($\gamma_n = 27.0$–27.7) enter from the south across 32S east of the Kermadec Ridge. At P11 the SEC transports 15.3 Sv of intermediate water and 22.9 Sv of thermocline water into the Coral Sea. (The SEC at P11 also carries about 13.9 Sv of water too light to appear at 32S, which participates in the tropical cell.) Within the uncertainty of these

estimates, the flows are similar and suggest that there is no need to convert a large volume of intermediate water to thermocline water within the subtropical Pacific north of 32S.

Schmitz also comments on a thick layer of fresh water ($S < 34.3$, and including both SAMW and AAIW) on 32S, which he suggests flows north across 32S to feed the export in the NGCUC. But only a very thin layer of water with $S < 34.3$ is found at 135W (Tsuchiya and Talley, 1996). The large pool of fresh water at 32S is apparently not carried around the subtropical gyre to cross 135W, or at least not without being substantially modified. An alternative view is that the large pool of fresh water on the eastern third of the 32S section recirculates, perhaps in the manner indicated by Reid (1986, 1997), and does not cross 135W. Based on Reid's circulation maps, the IW feeding the inflow to the Coral Sea, and ultimately the NGCUC, leaves the Southern Ocean between 130W and 160W. This suggestion is also consistent with the maps prepared with the SPAC data set (e.g. Figs. 6–10).

Tsuchiya and Talley (1996) find two varieties of AAIW at 135W. A light, fresh variety is found south of 17S, and a denser and more saline "equatorial" variety farther north. They suggest that the light variety is modified to greater density somewhere west of 135W, perhaps near the western boundary, because only the denser variety is found flowing through Vitiaz Strait to the tropics. We see no evidence of the lighter variety entering the Coral Sea across P11. A more "isopycnal" explanation of the two varieties of AAIW seen on 135W is that the very fresh, lighter variety recirculates in the South Pacific with little net export to the north and west. Water on the isopycnal corresponding to the equatorial variety of AAIW spreads north and west around the gyre, with its properties slowly modified by mixing along this path. The salinity minimum shifts to this level at latitudes north of the northern limit of the gyre which contains the recirculating, light variety of AAIW. That is, the shift in the density of the salinity minimum is not due to conversion of light salinity minimum water to dense salinity minimum water by mixing, but rather reflects a divergence of the circulation paths on these two isopycnals.

Our results suggest a pattern of intergyre and interbasin exchange that is more nearly isopycnal in character than suggested by Schmitz (1996) and Tsuchiya and Talley (1996). Our results agree with these earlier studies in suggesting that the mode and intermediate waters entering the Pacific from the south play an important role in the global interbasin circulation.

Our analysis is also relevant to exchanges between the Pacific and Indian Ocean taking place south of Australia. We find little evidence for significant net meridional flows through the southern Tasman Sea. The strong water property fronts near 36S suggest that little of the SAMW and AAIW entering from the south continues northward beyond this latitude. However, we do find support for export of modified subtropical water near the Tasmanian coast. We have identified an anticyclonic circulation in the southern Tasman Sea which brings southern waters northward, where they are modified by mixing with subtropical waters and then returned to the south. Rintoul and Sokolov (2000) use water mass distributions, geostrophic velocities, and ALACE float trajectories to show that this

outflow from the Tasman Sea continues to the west. Fine (1993) suggests this flow continues into the Indian Ocean. Taken together, this evidence suggests a transfer of heat and salt from the subtropical Pacific to the subtropical Indian Ocean which is mediated by eddy mixing in the southern Tasman Sea.

A number of questions remain. Our net eastward flow south of PNG matches the combined directly measured flow through Vitiaz Strait (15.8 Sv) and estimated flow at St Georges Channel (about 8 Sv). However, the inflow of intermediate water (10.8 Sv) is larger than previous estimates of the transport in this layer through Vitiaz Strait (2.2 Sv, Murray *et al.,* 1995; 2–4 Sv, Tsuchiya, 1991). Only a very thin layer of intermediate water is able to penetrate through the shallow Vitiaz Strait. Perhaps some intermediate water flows north through St Georges Channel or Solomon Strait, or there may be a local recirculation which carries some of this eastward flow back to the south to feed the northern branch of the SEC. In addition, given the match between our estimates of the NGCUC/NGCSC transport and the estimates in Vitiaz Strait and St Georges Channel, there is no way to accommodate a direct flow of water from the SEC through the Solomon Sea to these passages, as inferred by Andrews and Clegg (1989).

A more definitive statement regarding the intergyre exchange of intermediate water and the location of the diapycnal processes required to convert intermediate water to through-flow water awaits an analysis of the complete WOCE data set in the Pacific.

7. Summary

Our estimates of the circulation near the western boundary of the South Pacific are largely consistent with earlier estimates. However, the high vertical and horizontal resolution of this synoptic section allow the details of the flow to be refined and quantified in a way which was not possible with earlier data. Continuous profiles of oxygen, in particular, reveal a rich structure which illuminates the different flow paths crossing the section.

We have found that a deep reference level is most consistent with the water property distributions and mass conservation, both overall and in individual density layers. Relative to the deepest common depth, the SEC carries 55 Sv into the Coral Sea across P11. The SEC bifurcates at the Australian coast near 18S to form northward and southward flowing boundary currents of roughly equal magnitude. The northward branch forms the GBRUC and NGCUC; the southern branch feeds the EAC.

The SEC consists of three cores. The northern core carries 14 Sv of low oxygen thermocline and intermediate water as part of a tropical gyre. The gyre consists of eastward flow along the equator in the EUC, southward flow in the central Pacific, and westward flow in the northern branch of the SEC; equatorward flow in the low latitude western boundary current formed by the GBRUC/NGCUC closes the gyre in the west. A sharp oxygen front at 16S separates the northern core from the middle core, which carries high oxygen water as part of the subtropical gyre. About half (10 Sv) of the water carried west in the middle core of the SEC turns north and ultimately enters the NGCUC; the remainder

turns south to feed the EAC. The southern core of the SEC carries about 17 Sv of water similar in properties to that in the middle branch, all of which enters the EAC.

While the westward flow of the SEC extends throughout the water column, the transport is concentrated in the upper thermocline (the SLW). Two components of SLW identified by earlier authors are found at P11: a light, saline type formed in the central Pacific, and a dense, fresh type which we show to be formed in the Tasman Sea. Transport estimates in individual density layers suggest about 5 Sv of light northern SLW carried south by the EAC is converted to dense southern SLW by air-sea exchange. Lower thermocline waters (SAMW and AAIW) enter the Coral/Tasman seas farther south than the lighter SLW, due to the poleward shift with depth of the northern limb of the subtropical gyre.

Mass balance in the Coral Sea requires that about 29 Sv of the inflow from the SEC flows south in the EAC to the west of P11. Of the 57 Sv carried offshore by the EAC near 30S, 33 Sv recirculate south of 27S, and about 24 Sv is carried to the east. Additional recirculations at 25S (anticyclonic) and 23S (cyclonic) found at P11 are also found in many earlier dynamic topography maps and are likely to be standing gyres rather than transient eddies. Water properties along isopycnals are uniform in the Tasman Sea as a result of vigorous stirring by the eddy field.

A large anticyclinic eddy pinched off from the EAC is found at 33S, with a transport of about 60 Sv. Farther south the circulation is dominated by smaller, weaker eddies. An elongated anticyclonic circulation carries water into the Tasman Sea from the south near 155E, then west across P11, and finally back to the south near Tasmania, and plays an important part in introducing ''southern characteristics'' into the Tasman Sea. The net flow across P11 south of 30S is close to zero, and the water properties at all but the deepest levels suggest that the southern Tasman Sea is a cul de sac, across which there is little net meridional mean flow. However, eddy mixing in the southern Tasman Sea modifies the water entering from the south, introducing heat and salt from the subtropical Pacific, which is then returned to the Southern Ocean.

By quantifying the zonal flows entering and leaving the western boundary of the South Pacific, this study also provides some insight into the mechanisms involved in the exchange of water between Pacific and Indian Oceans. The transport in density layers across P11 is similar to estimates made farther "upstream" in the subtropical gyre at 30S. This suggests that the mode and intermediate waters which enter the Pacific from the south to compensate the Indonesian Throughflow are carried to the tropical western Pacific largely along isopycnals (although diapycnal mixing does modify the water mass properties). The conversion from dense to light water which must occur to supply the shallow throughflow apparently occurs in the tropical and/or North Pacific, rather than within the subtropical gyre of the South Pacific.

REFERENCES

Andrews, J. C. and S. Clegg. 1989. Coral Sea circulation and transport deducted from modal information models. Deep-Sea Res., *36,* 957–974.

Andrews, J. C., M. W. Lawrence and C. S. Nilsson. 1980. Observation of the Tasman Front. J. Phys. Oceanogr., *10,* 1854–1869.

Andrews, J. C. and P. Scully-Power. 1976. The structure of an East Australian Current anticyclonic eddy. J. Phys. Oceanogr., *6,* 756–765.

Boland, F. M. and J. A. Church. 1981. The East Australian Current, 1978. Deep-Sea Res., *28A,* 937–957.

Boland, F. M. and B. V. Hamon. 1970. The East Australian Current, 1965–1968. Deep-Sea Res., *17,* 777–794.

Burrage, D. M. 1993. Coral Sea currents. Corella, J. Aust. Bird Study Association, *17,* 135–145.

Butt, J. and E. Lindstrom. 1994. Currents off the east coast of New Ireland, Papua New Guinea, and their relevance to regional undercurrents in the Western Equatorial Pacific Ocean. J. Geophys. Res., *99,* 12503–12514.

Callahan, J. E. 1972. The structure and circulation of Deep Water in the Antarctic. Deep-Sea Res., *19,* 563–575.

Church, J. A. 1987. East Australian Current adjacent to the Great Barrier Reef. Aust. J. Mar. Freshwater Res., *38,* 671–683.

Church, J. A. and F. M. Boland. 1983. A permanent undercurrent adjacent to the Great Barrier Reef. J. Phys. Oceanogr., *13,* 1747–1749.

Deacon, G. E. R. 1937. The hydrology of the Southern Ocean. Discovery Reports, *15,* 3–122.

de Szoeke, R. A. 1987. On the wind-driven circulation of the South Pacific Ocean. J. Phys. Oceanogr., *17,* 613–630.

Donguy, J. R. 1994. Surface and subsurface salinity in the tropical Pacific Ocean. Relations with climate. Prog. Oceanogr., *34,* 45–78.

Donguy, J. R. and C. Henin. 1977. Origin of the Surface Tropical Water in the Coral and Tasman Seas. Aust. J. Mar. Freshwater Res., *28,* 321–332.

Donguy, J. R. and G. Meyers. 1996. Mean annual variations of transport of major currents in the tropical Pacific Ocean. Deep-Sea Res. I, *43,* 1105–1122.

Fine, R. A. 1993. Circulation of Antarctic Intermediate Water in the South Indian Ocean. Deep-Sea Res. I, *40,* 2021–2042.

Fine, R. A., R. Lukas, F. M. Bingham, M. J. Warner and R. H. Gammon. 1994. The western equatorial Pacific: A water mass crossroads. J. Geophys. Res., *99,* 25063–25080.

Garner, D. M. 1959. The subtropical convergence in New Zealand surface waters. N. Z. J. Geology Geophys., *2,* 315–337.

—— 1967. Hydrology of the south-east Tasman Sea. N. Z. Oceanogr. Inst. Memoir, *48,* 40 pp.

Godfrey, J. S. 1989. A Sverdrup model of the depth-integrated flow for the world ocean allowing for island circulations. Geophys. Astrophys. Fluid Dyn., *45,* 89–112.

Godfrey, J. S., G. R. Cresswell, T. J. Golding and A. F. Pearce. 1980. The separation of the East Australian Current. J. Phys. Oceanogr., *10,* 430–440.

Gordon, A. L. 1975. An Antarctic oceanographic section along 170°E. Deep-Sea Res., *22,* 357–377.

Gouretski, V. and K. Jancke. 1996. A new hydrographic data set for the South Pacific: synthesis of WOCE and historical data. SAC Technical Report No. 2, WOCE Report No. 143/96, (unpublished manuscript).

Hamon, B. V. 1965. The East Australian Current, 1960–1964. Deep-Sea Res., *12,* 899–921.

—— 1970. Western boundary currents in the South Pacific, *in* Scientific Exploration of the South Pacific, W. S. Wooster, ed., U.S. National Academy of Sciences, 51–59.

Heath, R. A. 1985. A review of the physical oceanography of the seas around New Zealand—1982. N. Z. J. Mar. Freshwater Res., *19,* 79–124.

Hellerman, S. and M. Rosenstein. 1983. Normal monthly wind stress over the World Ocean with error estimates. J. Phys. Oceanogr., *13,* 1093–1104.

Jackett, D. R. and T. J. McDougall. 1997. A neutral density variable for the world's oceans. J. Phys. Oceanogr., *27,* 237–263.

Johnson, G. C. and J. M. Toole. 1993. Flow of deep and bottom waters in the Pacific at 10°N. Deep-Sea Res. I, *40,* 371–394.

Kessler, W. S. and B. A. Taft. 1987. Dynamic heights and zonal geostrophic transport in the central Pacific during 1979–84. J. Phys. Oceanogr., *17,* 97–122.

Lilley, F. E. M., J. H. Filloux, N. L. Bindoff, I. J. Ferguson and P. J. Mulhearn. 1986. Barotropic flow of a warm-core ring from seafloor electric measurements. J. Geophys. Res., *91,* 12979–12984.

Lindstrom, E. J., J. Butt, R. Lukas and S. Godfrey. 1990. The flow through Vitiaz Strait and St. George's Channel, Papua New Guinea, *in* The Physical Oceanography of Sea Straits, L. J. Pratt, ed., NATO ASI Series C, *318,* Kluwer Academic Publishers, Boston, 171–189.

Lindstrom, E. J. and S. P. Hayes. 1989. Abyssal waters of the Coral and Solomon Seas. A contribution to the Klaus Wyrtki Symposium on ocean circulation and air-sea interaction, (unpublished manuscript).

Lindstrom, E. J., R. Lukas, R. Fine, E. Firing, S. Godfrey, G. Meyers and M. Tsuchiya. 1987. The Western Equatorial Pacific Ocean Circulation Study. Nature, *330,* 533–537.

Lozier, M. S., M. S. McCartney and W. B. Owens. 1994. Anomalous anomalies in averaged hydrographic data. J. Phys. Oceanogr., *24,* 2624–2638.

Lukas, R., T. Yamagata and J. P. McCreary. 1996. Pacific low-latitude western boundary currents and the Indonesian throughflow. J. Geophys. Res., *101,* 12209–12216.

McCartney, M. S. 1977. Subantarctic Mode Water. A Voyage of Discovery, supplement to Deep-Sea Res., George Deacon 70th Anniversary Volume, Martin Angel, ed., Pergamon Press, 103–119.

—— 1982. The subtropical recirculation of mode waters. J. Mar. Res., *40* (Supp.), 427–464.

McCartney, M. S. and M. O. Baringer. 1993. Notes on the S. Pacific hydrographic section near 32°S—WHP P6. WOCE Notes, *5,* 3–11.

Molinelli, E. J. 1981. The Antarctic influence on Antarctic intermediate water. J. Mar. Res., *39,* 267–293.

Morris, M., D. Roemmich and B. Cornuelle. 1996. Observation of variability in the South Pacific subtropical gyre. J. Phys. Oceanogr., *26,* 2359–2380.

Mulhearn, P. J., J. H. Filloux, F. E. M. Lilley, N. L. Bindoff and I. J. Ferguson. 1986. Abyssal currents during the formation and passage of a warm-core ring in the East Australian Current. Deep-Sea Res., *33,* 1563–1576.

—— 1988. Comparisons between surface, barotropic and abyssal flows during the passage of a warm-core ring. Aust. J. Mar. Freshwater Res., *39,* 697–707.

Murray, S., E. Lindstrom, J. Kindle and E. Weeks. 1995. Transport through the Vitiaz Strait. WOCE Notes, *7,* 21–23.

Nilsson, C. S., J. C. Andrews and P. Scully-Power. 1977. Observation of eddy formation off East Australia. J. Phys. Oceanogr., *7,* 659–669.

Nilsson, C. S. and G. R. Cresswell. 1981. The formation and evolution of East Australian Current warm-core eddies. Prog. Oceanogr., *9,* 133–183.

Picaut, J. and R. Tournier. 1991. Monitoring the 1979–1985 equatorial Pacific current transport with Expendable Bathythermography Data. J. Geophys. Res., *96* (Supp.), 3263–3277.

Reid, J. L., Jr. 1965. Intermediate Waters of the Pacific Ocean. Johns Hopkins Oceanographic Studies, *2,* 85 pp.

—— 1986. On the total geostrophic circulation of the South Pacific Ocean: flow patterns, tracers and transports. Prog. Oceanogr., *16,* 1–61.

—— 1997. On the total geostrophic circulation of the South Pacific Ocean: flow patterns, tracers and transports. Prog. Oceanogr., *39,* 263–352.

Reid, J. L. and R. J. Lynn. 1971. On the influence of the Norwegian-Greenland and Weddell seas upon the bottom waters of the Indian and Pacific oceans. Deep-Sea Res., *18,* 1063–1088.

Ridgway, K. R. and J. S. Godfrey. 1994. Mass and heat budgets in the East Australian Current: A direct approach. J. Geophys. Res., *99,* 3231–3248.

Rintoul, S. R. and J. L. Bullister. 1999. A late winter hydrographic section from Tasmania to Antarctica. Deep-Sea Res., *46,* 1417–1454.

Rintoul, S. and S. Sokolov. 2000. Baroclinic transport variability of the Antarctic Circumpolar Current south of Australia (WOCE repeat section SR3). J. Geophys. Res., (in press).

Rochford, D. J. 1968. The continuity of water masses along the western boundary of the Tasman and Coral Seas. Aust. J. Mar. Freshwater Res., *19,* 77–90.

Roemmich, D. and B. Cornuelle. 1992. The Subtropical Mode Waters of the South Pacific Ocean. J. Phys. Oceanogr., *22,* 1178–1187.

Roemmich, D., S. Hautala and D. Rudnick. 1996. Northward abyssal transport through the Samoan passage and adjacent regions. J. Geophys. Res., *101,* 14039–14055.

Rosenberg, M., R. Eriksen and S. Rintoul. 1995. Aurora Australis Marine Science Cruise AU9309/AU9391—Oceanographic field measurements and analysis. Research Report No. 2, Antarctic CRC, Hobart, Australia.

Schmitz, W. J., Jr. 1996. On the world ocean circulation: Volume II. The Pacific and Indian oceans/A global update. Woods Hole Oceanographic Institution Technical Report WHOI-96-08, 237 pp.

Schroeder, E., H. Stommel, D. Menzel and Sutcliff, Jr. 1959. Climatic stability of eighteen degree water at Bermuda. J. Geophys. Res., *64,* 363–366.

Scully-Power, P. D. 1973. Coral Sea flow budgets in winter. Aust. J. Mar. Freshwater Res., *24,* 203–215.

Sokolov, S. and S. R. Rintoul. 1999. Some remarks on interpolation of nonstationary oceanographic fields. J. Atmos. Oceanic Tech., *16,* 1434–1449.

Stanton, B. R. 1981. An oceanographic survey of the Tasman Front. N. Z. J. Mar. Freshwater Res., *15,* 289–297.

Stramma, L., R. G. Peterson and M. Tomczak. 1995. The South Pacific Current. J. Phys. Oceanogr., *25,* 77–91.

Taft, B. A., S. P. Hayes, G. E. Friederich and L. A. Codispoti. 1991. Flow of abyssal water into the Samoa Passage. Deep-Sea Res., *38*(Supp.), S103–S128.

Taft, B. A. and W. S. Kessler. 1991. Variations of zonal currents in the Central Tropical Pacific during 1970–1987: sea level and dynamic heights measurements. J. Geophys. Res., *96,* 12599–12618.

Thompson, R. O. R. Y. and R. J. Edwards. 1981. Mixing and water mass formation in the Australian subantarctic. J. Phys. Oceanogr., *11,* 1399–1407.

Thompson, R. O. R. Y. and G. Veronis. 1980. Transport calculations in the Tasman and Coral seas. Deep-Sea Res., *37A,* 303–323.

Toggweiler, J. R., K. Dixon and W. S. Broecker. 1991. The Peru upwelling and the ventilation of the South Pacific thermocline. J. Geophys. Res., *96,* 20467–20497.

Toole, J. M., S. E. Wijffels, M. S. McCartney, B. A. Warren, H. L. Bryden and J. A. Church. 1994. WOCE hydrographic section P6 across the subtropical South Pacific Ocean, *in* The Oceanographic Society, Pacific Basin Meeting, July 19–22, 1994, Honolulu, Hawaii, 76.

Toole, J. M., E. Zou and R. C. Millard. 1988. On the circulation of the upper waters in the western equatorial Pacific Ocean. Deep-Sea Res., *35,* 1451–1482.

Tsuchiya, M. 1981. The origin of the Pacific equatorial 13°C Water. J. Phys. Oceanogr., *11,* 794–812.

—— 1991. Flow path of the Antarctic Intermediate Water in the western equatorial South Pacific Ocean. Deep-Sea Res., *38* (Supp.), S273–S279.

Tsuchiya, M., R. Lukas, R. A. Fine, E. Firing and E. Lindstrom. 1989. Source waters of the Pacific Equatorial Undercurrent. Prog. Oceanogr., *23,* 101–147.

Tsuchiya, M. and L. D. Talley. 1996. Water-property distributions along an eastern Pacific hydrographic section at 135W. J. Mar. Res., *54,* 541–564.

Warren, B. A. 1970. General circulation of the South Pacific, *in* Scientific Exploration of the South Pacific, W. S. Wooster, ed., U.S. National Academy of Sciences, 33–49.

Warren, B. A. 1973. Transpacific hydrographic sections at Lats. 43°S and 28°C: The SCORPIO expedition—II. Deep water. Deep-Sea Res., *20,* 9–38.

Weare, B. C., P. T. Strub and M. D. Samuel. 1981. Annual mean surface heat fluxes in the tropical Pacific Ocean. J. Phys. Oceanogr., *11,* 705–717.

Wijffels, S. E., J. M. Toole and R. Davis. 2000. Revising the South Pacific subtropical circulation: a synthesis of WOCE observations along 32S. J. Geophys. Res. (submitted).

Worthington, L. V. 1959. The 18°C water in the Sargasso Sea. Deep-Sea Res., *5,* 297–305.

Wyrtki, K. 1960. The surface circulation in the Coral and Tasman seas. Div. Fish. Oceanogr. Tech. Paper No. 8, CSIRO, Australia, 44 pp.

—— 1961. The flow of water into the deep sea basins of the western South Pacific Ocean. Aust. J. Mar. Freshwater Res., *12,* 1–16.

—— 1962a. The subsurface water masses in the western South Pacific Ocean. Aust. J. Mar. Freshwater Res., *13,* 18–47.

—— 1962b. Geopotential topographies and associated circulation in the western South Pacific Ocean. Aust. J. Mar. Freshwater Res., *13,* 89–105.